NOVEL ASPECTS OF DIABETIC COMPLICATIONS: ALTERATIONS IN THE RESPIRATORY FUNCTION AND CEREBRAL INTEGRITY

Roberta Südy MD

PhD Thesis

Department of Anaesthesiology and Intensive Therapy

Department of Medical Physics and Informatics

University of Szeged, Hungary

Doctoral School of Multidisciplinary Medical Sciences

Supervisors:

Prof. Barna Babik MD PhD

Prof. Ferenc Petak PhD Dsc

Szeged, 2020

LIST OF SCIENTIFIC PUBLICATIONS INCLUDED IN THE PRESENT THESIS

I. **Differences between central venous and cerebral tissue oxygen saturation in anaesthetised patients with diabetes mellitus.**

Roberta Südy, Ferenc Peták, Álmos Schranc, Szilvia Agócs, Ivett Blaskovics, Csaba Lengyel, Barna Babik

Scientific reports, 2019 24;9(1):19740, doi: 10.1038/s41598-019-56221-4.

II. **Lung volume dependence of respiratory function in rodent models of diabetes mellitus**

Roberta Südy, Álmos Schranc, Gergely H. Fodor, József Tolnai, Barna Babik, Ferenc Peták

Respiratory Research, 2020 21(1): 82, doi: 10.1186/s12931-020-01334-y.

LIST OF SCIENTIFIC PUBLICATIONS RELATED TO THE SUBJECT OF THE PRESENT THESIS:

III. **Diabetes mellitus: endothelial dysfunction and changes in hemostasis**

Babik Babik, Peták Ferenc, Agócs Szilvia, Blaskovics Ivett, Alács Endre, Bodó Kinga, Südy Roberta

Orvosi Hetilap, 2018 159(33): 1335-1345, doi: 10.1556/650.2018.31130

LIST OF ABBREVIATIONS

AGEs	Advanced glycation end products
ANOVA	One-way analysis of variance
BBB	Blood brain barrier
CaO_2	Arterial oxygen content
CcO_2	Pulmonary end capillary oxygen content
CPB	Cardiopulmonary bypass
CPP	Cerebral perfusion pressure
$CrSO_2$	Cerebral tissue oxygen saturation
CvO_2	Central venous oxygen content
DM	Diabetes mellitus
EC	Extracellular
ECM	Extracellular matrix
eNOS	Endothelial nitric oxide synthase
ET-1	Endothelin-1
FOT	Forced oscillation technique
FRC	Functional residual capacity
G	Tissue damping
GFAT	Glutamine—fructose-6-phosphate aminotransferase
GSH	Reduced glutathione
GSSG	Glutathione disulphide
gSO_2	Difference between cerebral tissue and central venous oxygen saturation
H	Tissue elastance
HbA1c	Haemoglobin A1c
IC	Intracellular
IR	Insulin resistance
MAP	Mean arterial pressure
NADPH	Reduced nicotinamide adenine dinucleotide phosphate
NF-κB	Nuclear Factor Kappa B
NIRS	Near-infrared spectroscopy
NO	Nitrogen monoxide
OPCAB	Off-pump coronary artery bypass
PAI-1	Plasminogen activator inhibitor-1
$PaCO_2$	Partial pressures of carbon-dioxide in the arterial blood
PaO_2	Partial pressures of oxygen in the arterial blood
PEEP	Positive end expiratory pressure
PKC	Protein kinase C
Qs/Qt	Shunt fraction
RAGE	Receptor of advanced glycation end product
Raw	Airway resistance
RE, SE	Response and state entropy
ROCK	Rho-associated protein kinase
ROS	Reactive oxygen species
$ScvO_2$	Central venous oxygen saturation
STZ	Streptozotocin
T1DM	Type 1 diabetes mellitus
T2DM	Type 2 diabetes mellitus
TGF-β	Transforming growth factor-β
VEGF	Vascular endothelial growth factor
VSMC	Vascular smooth muscle cell

INTRODUCTION

Epidemiology and classification of diabetes mellitus

Diabetes mellitus (DM) is a heterogeneous disease characterised by hyperglycaemia and is among the diseases responsible for most of the morbidities and mortalities worldwide. Definitive diabetes affects nearly 8.5% of the total population [1], and 23.8 % of the disease might remain undiscovered [2]. The prevalence of DM doubled in the last three decades, meaning that 422 million people were affected in 2014, and 3.7 million people died because of diabetes or supra-normal blood sugar level [1].

In accordance with the WHO guideline of classification on DM [3] there are four main types of diabetes: type 1 diabetes (T1DM), type 2 diabetes (T2DM), other specific diabetes (*i.e.* monogenic diabetes) and diabetes associated with pregnancy. Ninety per cent of the patients have T2DM, where the most predisposing factors are obesity and an unhealthy lifestyle, which is leading to and enhancing the insulin resistance (IR). [4]. Most of the people affected by T2DM are overweight or obese based on the body mass index calculations. However, considerable number of patients diagnosed with T2DM are not reaching the threshold level of obesity by the BMI criteria, while they have a higher portion of body fat, mainly in the abdominal region [5]. In T1DM, both genetical and environmental factors can cause pancreatic β-cell loss and consequential absolute lack of insulin. T1DM develops mostly during childhood, but it can develop in adults as well. The previous autoimmune or non-autoimmune categories were rejected in the recent nomenclature [3].

Pathophysiology of diabetes mellitus

In diabetes, the pancreas β-cell dysfunction spread on a broad spectrum and progressing with time. Under physiological conditions, the insulin secretion is in balance with the insulin need due to the adaptation capability of the pancreatic β-cells. The relationship between β-cell function and the insulin sensitivity can be depicted as a hyperbola [6]. Deviation from the normal curve happens when the disease is in the phase of impaired glucose tolerance or the definitive T2DM stage. β-cells tend to produce more insulin to maintain the normal blood glucose level; this *circulous vitiousus* is leading to β-cell exhaustion. Despite the compensatory capacity of the β-cells, it has been shown that β-cells cannot renew themselves after 30 years of age [7].

Insulin resistance is a stage on the diabetes spectra when the tissues have a decreased response to a normal circulating level of insulin. Insulin resistance is frequently associated with various disorders, such as obesity, dyslipidaemia, and hypertension. There are pathologic changes in

insulin receptor isoforms, the insulin signalling pathway is damaged, and the amount of inflammatory molecules are increased in the stage of the insulin resistance. Under physiological conditions, the insulin increases the glucose uptake by the tissues — mostly by skeletal muscles — reduces its production in the liver, and the fat tissue is less likely to release fatty acids. Conversely, insulin resistance results in higher fatty acid levels and hyperglycaemia which lead to impaired feedback and further insulin resistance deterioration [6]. The progressive pathophysiological changes in glucose utilisation can lead to the development of T2DM characterised with a heterogeneous pattern of the glucose level in the body. Intracellular hypoglycaemia dominates 80% of the cells having insulin-dependent glucose transporters. In contrast there is a marked hyperglycaemia in the blood, and in the resting part of the cells having glucose transporters without a need of insulin, for instance, the endothelial cells, red blood cells, thrombocytes, pancreatic β-cells, renal glomerular cells.

Molecular mechanisms involved in the complications

The persistent intracellular hyperglycaemia activates cellular signalling pathway directly and through mitochondrial superoxide overproduction [8], causing intra- and extracellular damage. One of these mechanisms is the polyol pathway flux. Under physiological conditions, the aldose reductase enzyme turns the toxic aldehydes into inactive alcohols in the cell. The enzyme has a low affinity to glucose at normal glucose level. However, in intracellular hyperglycaemia, this enzyme acts as a catalysator for the reduced nicotinamide adenine dinucleotide phosphate (NADPH)-dependent reduction of glucose to sorbitol and at the end to fructose [9]. The lack in the given NADPH is resulting in a decreased production of reduced glutathione (GSH) from glutathione disulphide (GSSG). Since the NADPH is a crucial cofactor for the glutathione reductase enzyme, this phenomenon enhances the oxidative stress in the cell. Sorbitol molecules penetrate poorly through the cell membrane, thus the increased sorbitol level causing osmotic stress in the cell. Moreover, the metabolites of fructose enhance advanced glycation end products (AGEs) formation.

The formation of the AGEs leads to intracellular (IC) and extracellular (EC) protein damage and dysfunction. Abnormal interaction between the extracellular matrix (ECM) components and between the ECM components and integrins can occur due to AGEs damage [10]. Plasma proteins affected by AGEs-precursors preferably bind to AGEs receptors (RAGES), leading to enhanced reactive oxygen species (ROS) production. Moreover, this cascade results in pathological gene expression trough the Nuclear Factor Kappa B (NF-κB), which enhances the AGEs-formation [11].

In case of chronic intracellular hyperglycaemia fructose-6-phosphate molecules are likely to shunt the glycolytic pathway through the hexosamine pathway. Via an enzymatic modification by glutamine—fructose-6-phosphate aminotransferase (GFAT), fructose-6-phosphate is turning into glucosamine-6-phosphate and then uridine diphosphate N-acetyl glucosamine. Modification in gene expression by this pathway results in increased production of transforming growth factor-β (TGF-β and) and plasminogen activator inhibitor-1 (PAI-1) [12].

Furthermore, hyperglycaemia activates the protein kinase C (PKC) isoforms via elevating the intracellular diacyl-glycerol level. The hyperglycaemia induced PKC activation has several consequences on gene expression resulting in a plethora of pathological changes. The elevated level of the NAD(P)H oxidases enhances ROS activity, which activates further inflammatory cascades. Nevertheless, the NF-κB signalling plays a role in pro-inflammatory gene expression as well [13]. The increased TGF-β level results in capillary occlusion due to the higher amount of collagen and fibronectin in the vasculature [13]. In addition, the balance between the vasodilatory and vasoconstrictor factors is disturbed; the low endothelial nitric oxide synthase (eNOS) production is associated with concurrent overexpression of endothelin-1 (ET-1) [12, 14]. Furthermore, vascular permeability and angiogenesis are augmented due to the increased vascular endothelial grow factor (VEGF) level in smooth muscle cells [15]. Not only the endothelial cells and smooth muscle cells are affected by the PKC pathway, but the haemostasis is also disturbed via the elevated level of the PAI-1, resulting in decreased fibrinolysis [14].

All these mechanisms are interconnected, with numerous elements involved in more than one pathway (Fig 1.). The complex pathway networks in diabetes affect all organs in a very delicate way, connecting in several levels of action, enhancing its effects leading to endothelial and smooth muscle cell damage both on macro- and microvascular levels [16].
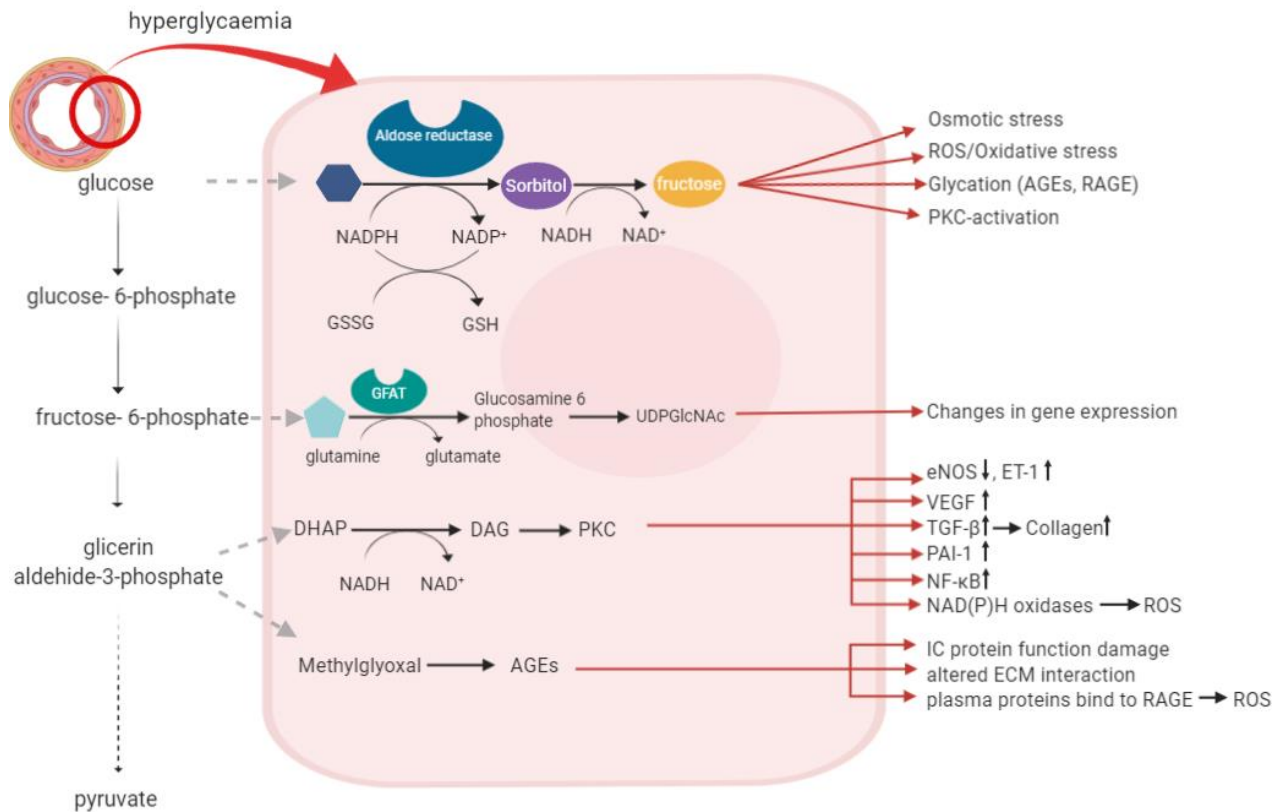
Fig 1. Schematic figure of the activated pathophysiological pathways in hyperglycaemia

Left: the main steps of the glycolysis, in the extracellular space pathophysiological pathways contributing to the diabetic complication. Right: the consequences of the activated pathways. High intracellular glucose level activating the polyol pathway flux resulting in fructose overproduction. The fructose-6-phosphate is shunting trough the hexosamine-pathway, while the higher amount of glicerin-aldehid-3-phostphate resulting in PKC activation and AGE formation. This figure was made in BioRender.

Abbreviations: NAD(P)H: Reduced nicotinamide adenine dinucleotide phosphate, GSSG: glutathione disulphide, GSH: reduced glutathione, GFAT: glutamine—fructose6-phosphate aminotransferase, UDPGlcNac: uridine diphosphate N-acetyl glucosamine:, DHAP: dihydroxyacetone phosphate, DAG: diacyl glycerol, PKC: protein kinase C, ROS: reactive oxygen species, AGEs: advanced glycation end products, RAGE: : advanced glycation end products receptor, eNOS: endothelial nitric oxide synthase, ET-1: Endothelin- 1, VEGF: vascular endothelial grow factor, TGF-β: of transforming growth factor-β, PAI-1: Plasminogen activator inhibitor-1, NF-κB: Nuclear Factor Kappa B IC: intracellular, ECM: extracellular matrix this figure was made in biorender

Multiorgan impairment in diabetes mellitus

The persistent hyperglycaemia in diabetes leads to an excessive amount of micro and macrovascular complications and multiorgan damage. One of the most common complications is diabetic retinopathy, which may start to progress even seven years before the diagnosis in T2DM [17]. A further complication is the development of diabetic nephropathy, which can lead to renal failure and chronic kidney injury and manifests as microalbuminuria or proteinuria. Diabetic neuropathy has different forms; however, the most common is the chronic sensorimotor distal symmetric polyneuropathy [18]. As a macrovascular consequence, atherosclerosis develops, and diabetes increases the risk of cardiovascular diseases, such as coronary heart disease and myocardial infarction. Moreover, the consequences of long-term hyperglycaemia and diabetes may potentially harm the cerebral and respiratory function as well [19-22].

Respiratory complications

The pathophysiological consequences of diabetes may also damage the pulmonary epithelium, bronchial smooth muscle cells beyond the vascular damage. Thus, the lungs can be among the organs most affected morphologically and functionally by this disease [19-21, 23, 24]. It has been reported that lung function deterioration might happen even three years ahead of the diagnosis of diabetes [25]. However, the reported consequences of diabetes on the lung function are conflicting, and the mechanisms have not been fully characterised. Abundant pathophysiological changes might play an important role in respiratory damage, such as IR, leptin resistance, low-grade inflammation, microvascular damage and neuropathy.

Long-term hyperglycaemia impairs the pulmonary vascular smooth muscle and endothelial cells resulting in elevated pulmonary vascular resistance, leading to decreased pulmonary blood flow and loss of pulmonary capillary blood volume [21]. Bronchial smooth muscle and pulmonary epithelial cells are affected by insulin resistance and low-grade inflammation [26] mostly via tumor necrosis factor α (TNF-α) activation and NF-κB signalling [27, 28]. The endothelial and epithelial dysfunction and ROS overproduction [29-31] contribute to the airway and lung parenchyma remodelling and alveolar wall thickening (79, 95). Furthermore, the altered pathways can manifest as sustained indirect and direct bronchial smooth muscle cell contraction [29, 30, 32, 33].

Since the lung is rich in elastin and collagen fibres, the ECM may also be a potential target for diabetes as alterations in the elastin–collagen matrix in the lung parenchyma [19, 34, 35] can occur. Thus, the above-detailed AGEs production and the AGEs-RAGES ligation might be abundant in

the lung. Type II pneumocyte damage results in decreased surfactant biosynthesis and secretion [36, 37] along with alveolocapillary barrier damage, thereby enhancing alveolar collapsibility and promoting lung derecruitment. Furthermore, leptin resistance might also contribute to respiratory complications through decreased alpha-1 antitrypsin and increased neutrophil elastase activity [38]. Diabetic autonomic neuropathy might also develop thus influencing the bronchomotor tone and airway responsiveness [39, 40]

While the effects of diabetes on the lung have been evidenced by these previous investigations, diverging results have been reported on the potential alterations in the lung function in the presence of this disease. Some studies have demonstrated declines in spirometry outcomes [41-44], whereas others found no detectable changes [45-48]. Possible explanations for this discrepancy include the dependence of spirometry results on the effort and cooperation of patients [49, 50], and substantial differences between study populations, such as the type and severity of DM, age, and comorbidities. Furthermore, forced expiratory parameters have limited sensitivity to detecting detrimental changes in lung tissue and peripheral airway mechanics [23, 45, 48], the aspects of the lung affected primarily by DM [48, 51]. The effects of DM on the mechanical properties of the lung tissue has been studied in an *ex vivo* experiment, and the results were limited to assess the elastic behaviour of the lung parenchyma [52].

Thus, it remains unclear how DM affects airway function and the viscoelastic mechanics of respiratory tissue, including its dissipative and elastic properties. It is also unknown whether DM influences the changes in mechanical parameters that occur with changes in lung volume.

Cerebral complication

The metabolic changes in diabetes deteriorate the brain function and structure insidiously in many ways, which can be attributed to the unique structure and physiology of the brain itself. Patients with diabetes have a higher risk of stroke (150-400%) with elevated stroke-related mortality [53] and the likelihood for dementia is around doubled [54]. The cerebral complications of diabetes have been studied intensively and they have led to clarification of several involved pathophysiological mechanisms. However, there is still lack of knowledge in fully understanding the cerebrovascular regulatory mechanism and consequences contributing to the organ failure.

Cerebral autoregulation under physiological condition

The brain has a high metabolic activity without energy reserve capacity and consumes about 20% of the total amount of oxygen available in the body. In addition, the brain depends on constant energy supply to meet the demand. Constant blood flow is required to maintain this fragile balance

[55]. Despite the physiological changes in systemic blood pressure, the cerebral blood flow is sustained by unique mechanisms such as the cerebrovascular autoregulation and the neurovascular coupling. Since the most powerful determinant of the flow in a vessel is its radius according to the Hagen-Poiseuille's law, these mechanisms involve mainly harmonised vasoconstriction and vasodilatation to maintain constant blood flow. Nevertheless, changing in vascular resistance can modify cerebral blood flow rapidly in order to support regional and overall demands of brain circulation [56]. Under physiological conditions, cerebrovascular autoregulation is maintained in a relatively wide range of cerebral perfusion pressure (CPP). If the CPP exceeds 160 mmHg or drops lower than 60 mmHg, the cerebral blood flow remains fairly constant [57].

In order to keep steady cerebral blood flow, vascular smooth muscle cells (VSMC) react against the different intramural pressures via myogenic response. Accordingly, the brain surface encompassed by the large pial arteries, and these arteries give nearly 50% of the total vascular resistance [58] compared to the vascular beds of other organs, where the myogenic response is determined by the small arteries [59, 60]. Nevertheless, studies describing that pial arteries respond to the negative feedback via the large-conductance calcium-activated potassium channels, but the penetrating arteries not. Interestingly, it was also reported that after ischemic insults myogenic dysfunction developed in the pial arteries [61] while the myogenic function of the penetrating arterioles remained intact [62].

The other mechanism contributes to the maintenance the energy and oxygen balance of the metabolically active brain regions is the neurovascular coupling. Neurovascular coupling is a feed-forward process where neuronal activation is translated to local vasodilation, called functional hyperaemia in the brain. Functional hyperaemia restores the depolarization-related lack of O_2 and ATP and preserves normal neuronal function. [63-65]. This mechanism obliges tight interaction in the neurovascular unit, which is composed of vascular cells, neurons and astrocytes. Vascular cells include endothelial cells, pericytes and VSMCs in pial and parenchymal arterioles in order to communicate with neurons. However, at the capillary level only pericytes and endothelial cells take part in the neurovascular unit [66].

Molecular and structural changes in diabetes mellitus

In diabetes, cerebral autoregulation might be impaired as a result of long term hyperglycaemia and compromised insulin signalling [67]. Increased cerebrovascular resistance and compromised blood flow occur due to the damaged myogenic response and dilatory mechanism. Endothelial dysfunction, morphological and functional changes are the key factors in impaired myogenic response. Intracellular hyperglycaemia induced polyol pathway and PKC activation resulting in

attenuated nitrogen monoxide (NO) release and increased ROS production. The decreased NO generation and biologic availability lead to further pro-inflammatory and inflammatory pathway activations. The decreased eNOS regulation is resulting in increased ET-1 production via TNF-α. [68-71]. Furthermore, the smooth muscle contraction might be prolonged and remarkable due to the phenotype changing of the VSMC [72] and the impaired Rho-associated protein kinase (ROCK) signal-induced increased myosin light-chain phosphorylation. [73-75].

Moreover, the hyperpolarization ability of ATP-sensitive potassium channels (K_{ATP}) are reported to be compromised by hyperglycaemia, which can also elevate the myogenic tone [76]. As an adaptive response to the modified haemodynamic conditions and hyperglycaemia, arteriogenesis and vascular remodelling may occur. Several factors might contribute to vascular remodelling, such as PKC-activation or matrix metalloprotease upregulation [77], which alters the vessel diameter, wall thickness and vessel density. Phenotype-changing, hypertrophy and proliferation of the VSMCs together with pathologic collagen deposition, play an important role in the cerebral complication of diabetes [78]. Moreover, pathological vasoregression appears due to oxidative stress and endothelial dysfunction [79]. In addition, extracellular AGEs induce apoptosis through the transcription factor Forkhead box protein O1 via ROS activation [80].

Diminished response to CO_2 [81-83] and thickened intima layer were observed in diabetes [84] resulting in diminished cerebrovascular reactivity. Hence, impaired cerebrovascular autoregulation manifests not only as an elevated myogenic tone but a reduced ability to constrict [74]. Furthermore, diabetes destructs blood brain barrier (BBB) resulting in increased BBB permeability [85], pericyte loss [86], thereby compromising cerebrovascular integrity with neurovascular uncoupling.

Since the brain is highly exposed to disturbances in the energy and oxygen supply, these pathophysiological changes can lead to a compromised oxygen balance in the cerebral tissue. Therefore, monitoring the changes in the regional oxygen balance in patients with diabetes may have particular importance. Despite the well-established molecular and functional changes in diabetes, there is still lack of knowledge on the cerebral regional oxygen saturation ($CrSO_2$), especially in anaesthetised patients in the perioperative period. Currently 30-40% of the patients undergoing cardiovascular surgeries have T2DM [87], which can partly be attributed to a therapeutic inertia in intensifying treatment of T2DM to reach optimal glycaemic, lipid and blood pressure control [88]. The structural and functional abnormalities in the vasculature [89] compromise adaptation mechanisms, subsequently increasing the risk of postoperative organ dysfunction,

including perioperative cerebral circulatory deficiency [90, 91]. The reduced vasodilatory reserve capacity increases the risk for a reduced cerebral tissue oxygen supply in T2DM patients, which may be responsible for the higher incidence of postoperative adverse neurocognitive dysfunction and stroke in the diabetic population [92-95]. Thus, it is particularly important to characterise the differences in $CrSO_2$ between the diabetic and non-diabetic patient population and follow the changes in $CrSO_2$ during the surgery. Moreover, in the perioperative period, the oxygen balance is routinely estimated from the oxygen saturation of central venous blood ($ScvO_2$) [96]. However, $ScvO_2$ reflects the overall oxygen balance [97]. Since substantial heterogeneity exists in oxygen extraction of various organs [98], the central venous oxygen saturation is not able to reflect regional changes of the tissue oxygenation.

HYPOTHESIS AND AIMS

The general aim of the present thesis was to extend our knowledge on the effect of diabetes on two distinct vital organs, the lung, and the brain in translational and clinical scenarios. A randomised controlled experimental study was performed to characterise the pulmonary effects of diabetes. This study design offered ideal conditions to reveal the adverse pulmonary mechanical consequences of diabetes without other confounding factors, such as the onset of the disease, age or comorbidities. Furthermore, well-controlled interventions with great translational value were feasible in this experimental model allowing the assessment of the volume-dependent behaviour of the lungs and the lung responsiveness in diabetes. The second study enclosed in the present thesis focused on the cerebral effect of diabetes in human subjects. Monitoring the regional differences in the tissue oxygen saturation is essential in a patient population with potentially compromised macro- and microcirculation, especially in the perioperative period. Since the cerebral circulation is disturbed in diabetes. and the brain is at risk of energy and oxygen supply deficit, we aimed at characterising the $CrSO_2$ in anaesthetised mechanically ventilated patients with diabetes during cardiac surgery.

Effect of diabetes on respiratory function: experimental study

The impact of diabetes on respiratory function has not yet been completely characterised. Changes in airway function and in the viscoelastic mechanical properties of the respiratory tissue remain unclear. Lack of knowledge continues to exist in the alterations of the airway and respiratory tissue mechanical parameters subsequent to changes in lung volume. Therefore, our aims in this study were to elucidate the effects of long-term hyperglycaemia on the respiratory system. Thus, we investigated the changes in the airway and respiratory tissue viscoelastic parameters with measurement techniques that allowed the exact characterization of these changes in well-established animal models of T1DM and T2DM. To address this aim, the following hypotheses were tested on the bases of theoretical considerations and previous findings:

I. Since the magnitude of the insults varies in the two groups with diabetes, we hypothesise differences in the respiratory outcomes between the type1 and type2 DM groups.

II. Deteriorations develop both in the dissipative and elastic components of respiratory tissue viscoelasticity.

III. The deteriorated airway function in diabetes results in changes in the airway responsiveness.

IV. The detrimental changes in respiratory function in T1DM and T2DM affect their changes with lung volume.

V. DM-induced functional and structural changes in the respiratory system are expected to result in loss of the lung volume, compromised gas exchange, and histological alteration. Thus, we investigated the functional residual capacity (FRC), fraction of arterial partial pressure of oxygen to the inspired fraction of oxygen (PaO_2/FiO_2), intrapulmonary shunt (Qs/Qt) and the amount of collagen in lung tissue samples.

Effects of diabetes on cerebral integrity: clinical study

The oxygen extraction rate of cerebral tissue is one of the highest in the body under physiological conditions [98], and substantial heterogeneity exists in oxygen extraction of various organs [98]. Therefore, the mixed venous oxygen saturation might not able to reflect regional changes in the tissue oxygenation and the cerebral tissue oxygen saturation derived from $ScvO_2$ can be overestimated [99]. Diabetic complications may compromise the cerebral tissue oxygen balance [100] and thus, estimation the intraoperative brain tissue oxygenation is particularly challenged in diabetic patients. Therefore, online monitoring of regional cerebral tissue oxygen saturation ($CrSO_2$) would have an advantage in T2DM patients in the intraoperative period to reveal hypoxemic episodes in the brain.

I. We hypothesise that the initial $CrSO_2$ measured by NIRS differs between patients with and without diabetes.

II. We hypothesise that the gap between $ScvO_2$ and $CrSO_2$ (gSO_2) is significantly widened in T2DM patients as a cardiovascular consequence of diabetes. Accordingly, $ScvO_2$ is not suitable to infer $CrSO_2$ in diabetic patients. To test this hypothesis, we aimed at comparing direct measurements of $CrSO_2$ using near-infrared spectroscopy (NIRS) to simultaneously obtained $ScvO_2$ data in patients with and without T2DM.

III. $ScvO_2$, $CrSO_2$ and gSO_2 are expected to exhibit intraoperative changes during cardiac surgery depending on the patient management with or without cardiopulmonary bypass (CPB). Thus, measurements were made during anaesthesia in two groups of cardiac surgery patients with or and without T2DM: those undergoing CPB and those scheduled for off-pump coronary artery bypass (OPCAB) grafting procedure.

MATERIALS AND METHODS

Methods in the experimental study

Ethics

This study was approved by the National Food Chain Safety and Animal Health Directorate of Csongrád County, Hungary (no. XXXII./2098/2018), on September 24, 2018. The procedures were implemented in compliance with the guidelines of the Scientific Committee of Animal Experimentation of the Hungarian Academy of Sciences (updated Law and Regulations on Animal Protection: 40/2013. [II. 14.], the Government of Hungary), and European Union Directive 2010/63/EU on the protection of animals used for scientific purposes. The results were reported in line with the ARRIVE guidelines.

Inducing diabetes

The study used 5-week-old male Wistar rats (mean weight ± 95% confidence interval, 187.3 ± 3.7 g, n = 42). During the initial phase of the study protocol, the animals were housed for 15 weeks under close daily observation in accordance with the animal welfare assessment and 3R guidelines. Well-validated models were adapted to induce models of type 1 and type 2 DM, with proven hyperglycaemia, insulin resistance, and the diffuse degeneration of pancreatic cells [101-106]. The 5-week-old rats were assigned randomly to three protocol groups: model of type 1 DM (DM1 group, n = 14), model of type 2 DM (DM2 group, n = 14), and control group (n = 14). They were fed in accordance with their group allocations (Fig 2): rats in the DM1 and control groups received a normal diet (fat and protein contents of 3.9% and 20.1%, respectively), whereas those allocated to the DM2 group were fed a high-fat diet (Altromin C1080, 47% fat, 18% protein, 35% carbohydrate; Altromin Spezialfutter GmbH & Co. KG, Lage, Germany). After a 3-week period (at the age of 8 weeks), the DM1 group rats were treated with a single high dose of streptozotocin (STZ, 65 mg/kg) [101, 105], the DM2 group rats were treated with a low dose (30 mg/kg) of STZ [102-104, 106], and the controls received the vehicle of the STZ (citrate buffer, pH 4.4). Before the injection of STZ or vehicle and 1 week after the treatment (age of 9 weeks), fasting glucose levels were measured from the tail vein using an Accu-Chek Active blood glucose meter (Roche, Basel, Switzerland). Four rats in the DM2 group were administered a second injection of 30 mg/kg STZ treatment because their fasting glucose level was <7.8 mmol/l [103, 106]. One animal in the DM1 group was sacrificed after 7 weeks due to isolation and its unsatisfactory health condition.
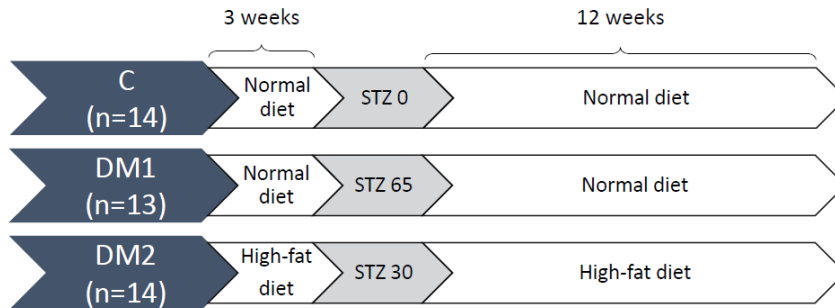
Figure 2: Scheme summarizing the treatment *Three groups of animals received different treatments according to their group allocations. The animals in DM1 and in C groups received normal diet, while the rats in the DM2 group were fed with high-fat diet. After the three-week pretreatment period animals in the DM1 group received high-dose intraperitoneal streptozotocin. Rats in the DM2 group received low dose streptozotocin. Abbreviations: **DM1:** model of type 1 diabetes, **DM2:** model of type 2 diabetes, **C:** control group; **STZ:** streptozotocin in mg/kg*

Animal preparations

The experiments were performed on week 16 (age of 20 weeks). Anaesthesia was induced by an intraperitoneal injection of sodium pentobarbital (45 mg/kg, Sigma-Aldrich, Budapest, Hungary). After administering local anaesthesia (subcutaneous lidocaine, 2–4 mg/kg), a polyethylene cannula with an inner diameter of 18G was inserted into the trachea through a tracheostomy. The tracheal cannula was connected to a small animal ventilator (Model 683; Harvard Apparatus, South Natick, MA, USA), and the animal was mechanically ventilated (55-60 breaths/min, tidal volume 7 ml/kg, with a fraction of inspired oxygen [FiO_2] of 21%). The femoral artery was catheterised for blood pressure measurements and the collection of blood samples. The femoral vein was cannulated for drug administration and the jugular vein was secured for drug administration and the collection of venous blood samples. Anaesthesia was maintained with pentobarbital (5 mg/kg, intravenous (iv.), every 30 min). The rat was placed on a heating pad (model 507223F; Harvard Apparatus, Holliston, MA, USA) and its body temperature was maintained at 37 ± 0.5 °C. The forced oscillation measurements to evaluate the impedance of the respiratory system were made under neuromuscular blockade, achieved by the repeated iv. administration of pipecuronium (0.1 mg/kg every 30 min; Arduan, Richter-Gedeon, Budapest, Hungary).

Measurement of functional residual capacity

The FRC was measured as described previously [107]. Briefly, the rat was tracheostomised and placed in a whole-body plethysmography box (Fig 3.). The trachea and box were closed at end-expiration and the measurements were made while the animal generated breathing efforts against the closed trachea. The FRC was calculated from the simultaneously measured tracheal and box pressure signals by applying the Boyle–Mariotte law [107].
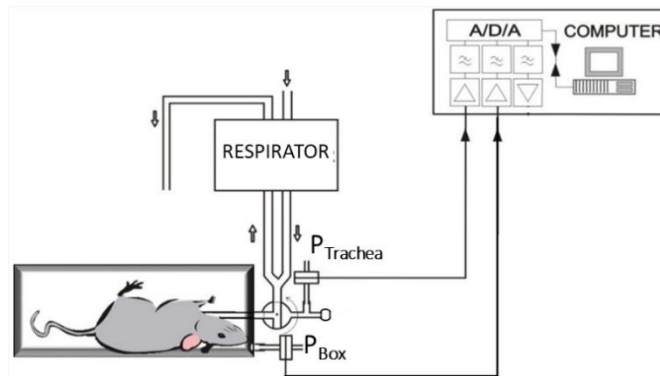

Figure 3. Scheme of the measurement apparatus for the assessment of the functional residual capacity. $P_{trachea}$ and P_{box} indicate the pressure sensors at the tracheal canula and at the whole-body plethysmography box, respectively.

Measuring airway and respiratory tissue mechanics

The input impedance of the respiratory system (Zrs) was measured by the forced oscillation technique, as described previously [108]. Briefly, the tracheal cannula was connected to a loudspeaker-in-box system, while ventilation was suspended at end-expiration. A small-amplitude pseudorandom signal (<1.5 cmH$_2$O, with 23 non-integer multiple-frequency components between 0.5 and 20.75 Hz) was applied to the tracheal cannula through a wave tube (polyethylene; length 100 cm, internal diameter 2 mm). To maintain uniform transpulmonary pressure during the measurements, the pressure in the loudspeaker box was set to be equivalent to that of the positive end-expiratory pressure (PEEP) used for that experiment (0, 3, or 6 cmH$_2$O). During 8-s measurement periods, pressures were measured simultaneously at the loudspeaker and tracheal ends of the wave tube with miniature differential pressure transducers (Honeywell Differential Pressure Sensor model 24PCEFA6D; Honeywell, Charlotte, NC, USA). Zrs was calculated as the load impedance of the wave tube [108]. At least four technically acceptable measurements were made at each stage of the protocol. The mechanical properties of the respiratory system were characterised by fitting a well-validated model [109] to the averaged Zrs spectra. The model comprised frequency-independent airway resistance (Raw) and airway inertance in series with a viscoelastic constant-phase tissue unit [109], and incorporated tissue damping (G) and elastance

(H). Tissue histeresivity (η), which characterises the coupling between the dissipative and elastic forces within the respiratory tissues was calculated as G/H [110].
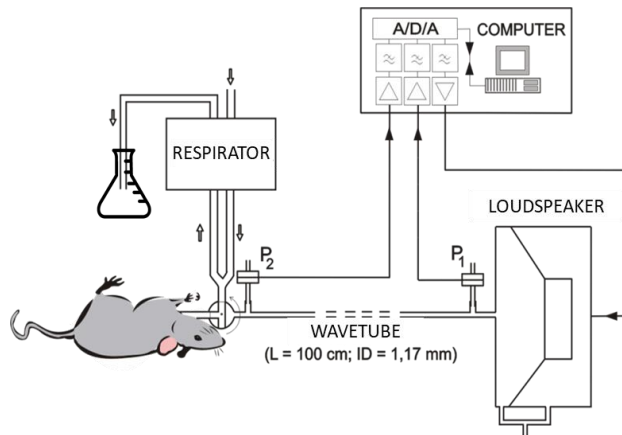

Figure 4. Scheme of the forced oscillatory measurement apparatus
P_1 and P_2 indicate the miniature pressure sensors at the loudspeaker and at the tracheal end of the wave tube, respectively. During the measurements, the respiratory limb was closed, and the animal was connected to the loudspeaker via the wave tube. Between the measurements oscillatory circuit was closed and the respiratory limb was open. The Erlenmeyer flask filled with water was used to generate PEEP

Measurement of intrapulmonary shunt fraction and oxygenation

For the blood gas analyses, 0.1-ml samples of arterial and central venous blood were collected simultaneously. The capillary (CcO_2), arterial (CaO_2), and venous (CvO_2) oxygen contents were evaluated from the blood gases and used to calculate the intrapulmonary shunt fraction (Qs/Qt) by applying the modified Berggren equation [111]:

$$\frac{Q_s}{Q_t} = \frac{CcO_2 - CaO_2}{CcO_2 - CvO_2}$$

To characterise the oxygenation efficiency PaO_2/FiO_2 was calculated from the arterial blood gas assessments.

Lung tissue histology

After completing the experimental protocol, a midline thoracotomy was performed, and the lungs were fixed by introducing 4% formaldehyde via the tracheal cannula with a hydrostatic pressure of 20 cmH_2O. The heart-lung blocks were then removed in one piece from the thoracic cavity. To visualise the collagen in the lung, tissue samples were fixed in 4% buffered formalin, embedded in paraffin, and 5-μm tissue sections were stained with Picro Sirius Red staining (Sigma-Aldrich). These were scanned with a Zeiss Mirax MIDI slide scanner at a magnification of $\times$20. At least

three representative 0.15-mm^2 sized rectangular regions of interest that contained alveoli without bronchi or large vessels were analysed in each section. The collagen was segmented and quantified in the lung tissue sections by using the Trainable Weka Segmentation plugin in Fiji software [112]. The histological analyses were made by one person who was blinded for the group allocation.

Experimental protocol

collThe experimental protocol is summarised in Fig 5. Following a 12-week housing period after the induction of DM (at the age of 20 weeks), each rat was anesthetised, and the trachea was secured. The FRC was measured, followed by the surgical insertion of the arterial and venous catheters. Animals were initially ventilated with a PEEP of 3 cmH$_2$O. A hyperinflation manoeuvre was then performed to standardise the volume history. After 3 min, arterial and venous blood gas samples were taken simultaneously and the first set of set of Zrs were collected. Blood gas analyses and Zrs measurements were made at PEEP levels of 0 and 6 cmH$_2$O, in random order. A period of 3 min was allowed for the animal after each PEEP step to maintain a steady state condition during the data collection. After completing the study on characterizing the PEEP-dependence, the PEEP was fixed at 3 cmH$_2$O and a set of Zrs data was collected to establish the baseline for the bronchoprovocation tests with doubling doses (2, 4, 8, 16, and 32 µg/kg/min) of iv methacholine (MCh). At each MCh dose, steady-state bronchoconstriction was established (defined as <5% difference in Raw between consecutive measurements) and forced oscillation Zrs data were measured. After completing the measurement protocol, each animal was euthanised by an overdose of pentobarbital and the lungs were removed for histological analysis.
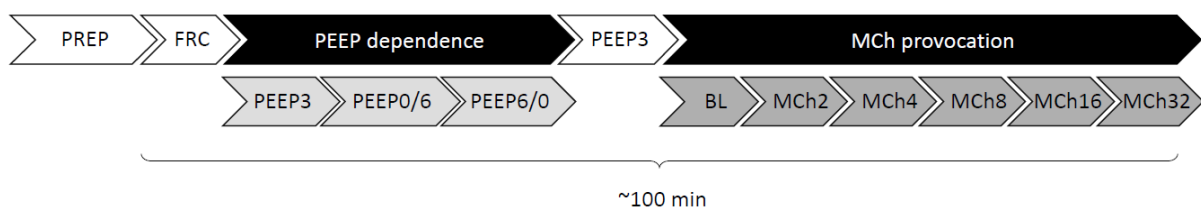
Figure 5. Schemes summarizing the experimental protocol (B). *After 12 weeks, forced oscillation measurements and blood gas analyzes were performed at three different positive end-expiratory pressures (0, 3, and 6 cmH$_2$O:* ***PEEP0, PEEP3,*** *and* ***PEEP6,*** *respectively). Forced oscillation respiratory mechanics were assessed at a PEEP of 3 cmH$_2$O during provocation tests with increasing doses (2-32 µg/kg/min) of methacholine (****MCh****) following the baseline measurement (****BL****). Further abbreviations:* ***FRC:*** *measurement of functional residual capacity,* ***PREP:*** *animal preparations*

Methods in the clinical study

Patients

Hundred thirty-nine consecutive patients with T2DM (n=48) and control (C) subjects without T2DM (n=91) undergoing cardiac surgery were enrolled in this prospective descriptive cohort study. Patients were defined as having T2DM if their medical history included a diagnosis of T2DM and haemoglobin A1c (HbA1c) > 6.4%. All patients underwent either OPCAB (C-OPCAB, n=31 and T2DM-OPCAB, n=24) or CPB (C-CPB, n=60, T2DM-CPB, n=24). Patients older than 80 years of age or with poor ejection fraction (<40%), unilateral internal carotid stenosis (>75%), or medical history of smoking, chronic obstructive pulmonary disease or stroke were excluded from the study. The protocol was approved by the Human Research Ethics Committee of Szeged University, Hungary (no. WHO 2788), and the patients gave their informed consent to participation in the study. The study was performed in accordance with the ethical standards laid down in the 1964 Declaration of Helsinki and its later amendments.

Anaesthesia

One hour before the surgery, patients were premedicated with lorazepam (per os, 2.5 mg). Before induction of anaesthesia, the NIRS sensors (INVOS 3100, Somanetics, MI, USA) were positioned on both sides of the forehead. Sensors to detect depth of anaesthesia were also mounted on the forehead to monitor EMG and EEG activities. These signals were used to calculate response (RE) and state entropy (SE), respectively (GE Healthcare, Chicago, USA). Induction of anaesthesia was achieved by iv midazolam (30 µg/kg), sufentanil (0.4–0.5 µg/kg), and propofol (0.3–0.5 mg/kg), and iv propofol (50 µg/kg/min) was administered to maintain anaesthesia. Intravenous boluses of rocuronium (0.6 mg/kg for induction and 0.2 mg/kg every 30 minutes for maintenance) was administered iv to ensure neuromuscular blockade. A cuffed tracheal tube (internal diameter of 7, 8, or 9 mm) was used for tracheal intubation, and patients were mechanically ventilated (Dräger Zeus, Lübeck, Germany) in volume-controlled mode with decelerating flow. A tidal volume of 7 ml/kg and a positive end-expiratory pressure of 4 cmH$_2$O were applied, and the ventilation frequency was adjusted to 12–14 breaths/min to maintain end-tidal CO$_2$ partial pressure of 36-38 mmHg. Mechanical ventilation was performed with a fraction of inspired oxygen of 0.5 during the entire OPCAB procedure and before CPB, and it was increased to 0.8 after CPB. As a standard part of the cardiac anaesthesia procedure, oesophageal and rectal temperature probes were introduced, and a central venous line was inserted into the right jugular vein. The left radial artery was also cannulated to monitor systolic, diastolic and mean arterial (MAP) blood pressures and arterial blood gas samples.

The membrane oxygenator was primed with 1,500 ml lactated Ringer's solution prior to CPB. Intravenous heparin (150 or 300 U/kg for OPCAB and CPB procedures, respectively) was injected into the patient, and an activated clotting time of 300 s was achieved during OPCAB and of 400 s during CPB procedures. During CPB, mild hypothermia was allowed, the mechanical ventilation was stopped, and the ventilator was disconnected without applying positive airway pressure. Before restoring ventilation, the lungs were inflated 3–5 times to a peak airway pressure of 30 cmH_2O to facilitate lung recruitment. Normothermia was maintained in the OPCAB patients.

Measurement of cerebral-tissue oxygen saturation

The spatially resolved continuous-wave NIRS technique was applied to estimate $CrSO_2$. This monitor uses two different wavelengths (730 and 810 nm) and has two detectors positioned 3 and 4 cm from the light source. Computing the differences between the intensity of the emitted and the reflected light [113] with two receivers [114] allows the measurement of the oxygen saturation of the cerebral cortex. In this study, two adult sensors were applied on the left and right sides of the patient's forehead symmetrically, placed more than 3 cm from the superior rim of the orbit [115].The cerebral-tissue oxygen saturation was monitored continuously during the surgical procedures and the data were registered in each protocol stage. The mean value of the $CrSO_2$ measured by the sensors was calculated for each protocol stage and used for further analyses.

Measurement of central venous oxygen saturation

The $ScvO_2$ was measured from central venous blood samples (Radiometer ABL 505, Copenhagen, Denmark). The proper positioning of the central venous catheter was verified by the surgeon via manually palpating the catheter tip. The partial pressures of oxygen (PaO_2) and carbon-dioxide ($PaCO_2$), haemoglobin, pH and oxygen content (CaO_2) were determined from arterial blood gas samples at each protocol stage.

Measurement protocol

The scheme of the measurement protocol is outlined on Fig 5. After securing arterial and peripheral venous lines and placement of NIRS and entropy sensors, data collection was initiated immediately before anaesthesia induction in all groups of patients. Since catheterization of the jugular vein was scheduled after anaesthesia induction, $ScvO_2$ and gSO_2 data were not available at the first protocol stage. After anaesthesia induction and muscle relaxation, all measurements were repeated before surgical incision. For the patients undergoing CPB procedures, the whole data set was registered at the beginning of CPB after clamping the aorta and 5 min before the end of CPB. For the patients undergoing OPCAB procedures, collection of the full set of data was performed during performance of the first proximal anastomosis between the aorta and saphenous vein graft. The final stage of the protocol was allocated to the end of the operation after sternal closure. All invasive (i.e. arterial and venous blood gas) and non-invasive data were registered simultaneously at each protocol stage after ensuring a 3 min stead-state condition.
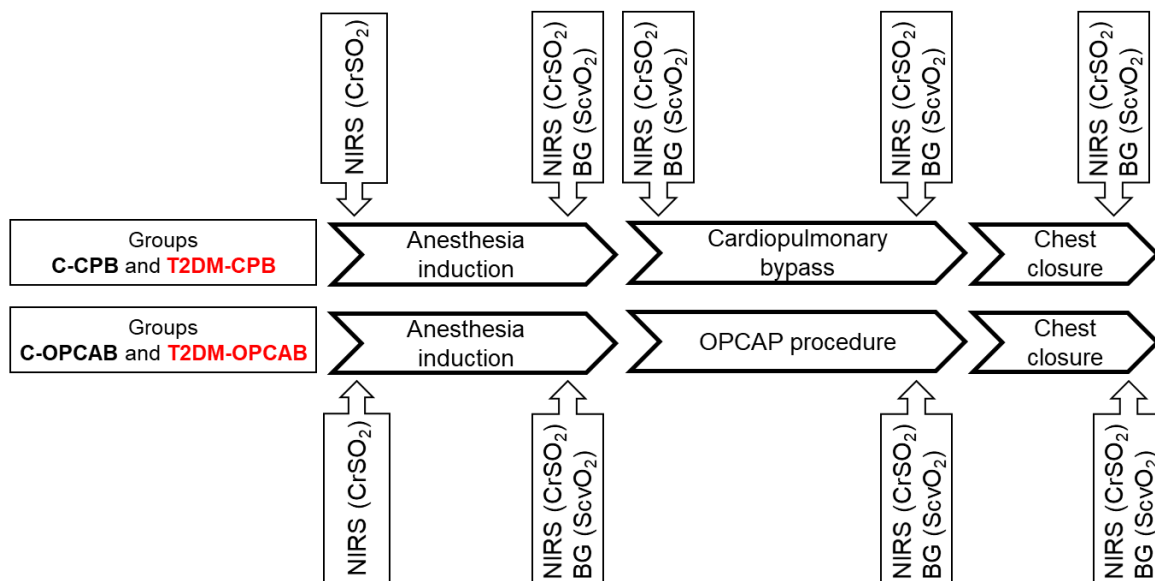
*Figure 6. The scheme of the measurement protocol. Measurements were made at five time points in the patients with cardiac surgeries requiring cardiopulmonary bypass (**Groups C-CPB** and **T2DM-CPB**), while four measurements were performed in the patients with off-pump coronary bypass grafting surgeries (**C-OPCAB** and **T2DM-OPCAB**). Cerebral tissue oxygen saturation (**CrSO₂**) measured by near infrared spectroscopy (**NIRS**). Central venous oxygen saturation (**ScvO₂**) determined from blood gas analyses (**BG**).*

Statistical analyses

In the animal study, data are expressed as mean ± standard deviation (SD) for normally distributed variables, and median with interquartile range (1st - 3rd quartile) otherwise. The Kolmogorov–Smirnov test was used to test data distributions for normality; where necessary, a logarithmic transformation was performed to normalise the data. Two-way repeated-measures analysis of variance (ANOVA) with Holm–Sidak *post hoc* analyses were used to assess the effects of the PEEP and group allocation on the respiratory mechanical and oxygenation parameters. Between group differences in airway responsiveness to MCh were evaluated with further two-way repeated-measures ANOVA with Holm–Sidak *post hoc* analyses. The MCh doses that elicited a 50% increase in Raw relative to baseline (PD_{50}) were determined by fitting linear models to the individual dose–response curves. One-way ANOVA with Dunn's *post hoc* analyses was used to evaluate the differences between groups in body weights, blood glucose levels, specific airway and respiratory tissue parameters, PD_{50}, and the results of the histological analysis. Correlation between the collagen expression in the lung tissue and viscoelastic properties of the respiratory system was determined by the Pearson correlation analysis.

In the clinical study for numerically reported data, the scatters in measured variables are expressed as 95% confidence interval for the mean. The normality of the data was verified with the Shapiro-Wilk test; one-way analysis of variance (ANOVA) was used to test differences in the demographic, anthropometric, and clinical characteristics of the patients when they were included in the control, and diabetic groups. Fisher's exact test was performed to assess the differences in the surgical procedures between the protocol groups. Pearson's correlation test was applied to assess the relationship between global and regional oxygen saturation indices. Two-way repeated measures ANOVA with the inclusion of an interaction term was used for all measured variables with the protocol stage as within-subject factor (protocol stages) and group allocation as between-subject factor to establish the effects of T2DM and the surgical procedure on the oxygen saturation indices. The Holm–Sidak multiple comparison procedure was adopted to compare the variables in the study groups at different protocol stages. Further two-way repeated measures ANOVA tests were applied to assess between-group and within-group differences in the parameters influencing cerebral-tissue oxygen saturation.

Sample size estimations were performed for both studies. In the experimental study the sample size estimation for the repeated-measures ANOVA for the variable Raw, with a power of 0.8 and alpha of 0.05. indicated that at least 10 animals were required in each group to detect a statistically significant difference [116]. In the clinical study sample sizes were estimated to enable the detection of a 10% difference in the primary outcome parameter gSO_2 that we considered clinically

significant. Accordingly, sample-size estimation based on an ANOVA test with four groups of patients indicated that 24 patients were required in each group to detect a significant difference between the protocol groups (the assumed variability of 10%, power of 0.8 and alpha of 0.05). Due to the prevalence of T2DM in cardiac surgery, this targeted number of T2DM patients resulted in twofold number of the patients without diabetes.

The statistical tests were performed with the SigmaPlot statistical software package (Version 13, Systat Software, Inc., Chicago, IL, USA) and R environment. All reported p values are two-sided, and the statistical tests were performed with a significance level of $p < 0.05$.

RESULTS

Effects of diabetes on the respiratory system: results in the experimental study

Initial parameters after the treatment period

Body weights, serum glucose levels, and the initial lung function parameters for the control and STZ-treated rats are summarised in Table 1. At the end of the 12-week treatment period, the mean body weight in the rats of the DM1 group was significantly lower than those in the DM2 and control groups. Significant elevations in blood glucose level were observed in the rats of the DM1 and DM2 groups compared to the control animals. The FRC measurements showed a significant reduction in static lung volume in the DM1 group rats; however, when the FRC values were normalised to body weight, they were significantly higher for the DM1 group rats than for those in the other two groups. Specific airway and respiratory tissue parameters were significantly higher in the DM1 and DM2 groups than in the control group.

	Group C (n=14)	Group DM1 (N=13)	Group DM2 (N=14)	p
Body weight (g)	563±49	348±91[*]	529±76[#]	<0.001
Blood glucose (mmol/l)	5.8 (5.6-6.1)	29.9(25.75-35)[*]	14.75(7.0-27.3)[*]	<0.001
FRC (ml)	4.3±0.5	3.6±0.6[*]	4.4±0.8[#]	0.003
FRC$_N$ (ml/kg)	7.5(6.8-8.7)	10.2 (8.6-11.3)[*]	8.1(6.7-9.3)[#]	0.003
SRaw (cmH$_2$O.s)	0.23(0.19-0.24)	0.27(0.24-0.32)[*]	0.27(0.23-0.34)[*]	0.004
SG (cmH$_2$O)	3.1(2.7-3.3)	3.4(3.2-4.0)[*]	3.6(3.0-4.4)[*]	0.023
SH (cmH$_2$O)	12.0±2.7	17.3±4.9[*]	17.2±5.8[*]	0.007

*Table 1. Main outcome parameters: In the control rats (**Group C**) and in model of type 1 (**Group DM1**) and type 2 (**Group DM2**) diabetes mellitus presented as mean±SD (Body weight, FRC and SH) and median (Q1,Q3), (Blood glucose, FRC$_N$, SRaw, SG) . **FRC**: functional residual capacity, **FRC$_N$**: functional residual capacity normalised to body weight (**FRC/BW**), **SRaw:** specific airway resistance (**Raw × FRC**), **SG:** specific respiratory tissue damping (**G × FRC**), **SH**: specific airway resistance (**H × FRC**); all obtained without applying positive end-expiratory pressure. **p:** results of the one-way ANOVA tests and ANOVA on ranks. *: p<0.05 vs. Group C, #: p<0.05 between Groups DM2 and DM1 by using Dunn's post-hoc analyses.*

Changes in the respiratory mechanical properties

Fig 7 shows how the airway and viscoelastic parameters of the respiratory tissues varied with the PEEP for the three groups. Raw was significantly greater in both groups of diabetic animals than in the control group at all PEEP levels ($p < 0.001$). Two-way ANOVAs showed significant interactions between group and PEEP level for the parameters G ($p < 0.001$) and H ($p < 0.001$), indicating that the treatment affected these parameters' dependence on PEEP. The dissipative properties of the respiratory tissues reflected by G were significantly compromised in the DM1 group when PEEP = 0 cmH$_2$O. The respiratory tissue stiffness was elevated in both the DM1 ($p < 0.001$) and the DM2 ($p = 0.039$) groups at all PEEP levels, with more pronounced differences at low lung volumes. The dissociated PEEP dependences of G and H resulted in changes in η that varied between the groups, with significant decreases observed in the DM1 group for all three levels of PEEP ($p < 0.001$) and in the DM2 group when the PEEP was 3 or 6 cmH$_2$O ($p = 0.014$) compared to the control group.
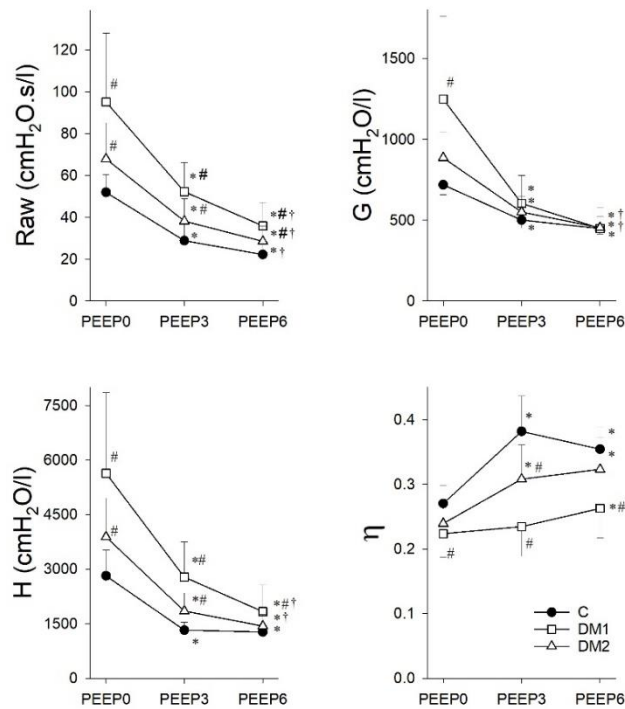
Figure 7. Airway and viscoelastic respiratory tissue mechanical parameters. Measurements obtained at positive end-expiratory pressures of 0, 3, and 6 cmH$_2$O (PEEP0, PEEP3, and PEEP6, respectively) in control rats (closed circles, C, n = 14) and in rats in the type 1 diabetes (DM1, open squares, n = 13) and type 2 diabetes (DM2, open triangles, n = 14) groups. The symbols and error bars represent the mean and SD values, respectively. * p < 0.05 vs. PEEP0 within a group; † p < 0.05 vs. PEEP3; # p < 0.05 vs. C within a PEEP. Abbreviations: Raw, airway resistance; G, tissue damping (resistance); H, tissue elastance; η, tissue histeresivity η= G/H. C within a condition; † p < 0.05 vs. DM2 within a condition.

Airway response to Metacholine

Airway resistance and its absolute (right) and relative (left) changes to the baseline (BL) during the MCh provocation tests are shown in Fig 8. Significant elevations in the basal Raw values were observed in the DM1 (p<0.001) and DM2 (p<0.05) groups. These differences remained at the lower doses of MCh, whereas the absolute value of Raw became significantly lower in the DM1 rats at the highest dose of MCh (p<0.05). Due to the significantly higher baseline Raw values in the diabetic rats, the differences in the dose-response curves to MCh between the protocol groups is more obvious when the responses are expressed as relative changes to baseline (right). In the control and DM2 groups, elevations in Raw were statistically significant from the 8 µg/kg/min MCh dose (p < 0.05), whereas in the DM1 group this increase was only observed after 16 µg/kg/min (p < 0.05). At the highest MCh dose, the MCh-induced relative increases in Raw were significantly lower in both DM1 and DM2 groups compared to control (p = 0.001). The characteristic shifts in the dose-response curves showed that the PD_{50} for MCh was significantly higher for the DM1 group (25.3 ± 20 µg/kg/min) than for the control group (8.9 ± 3.3 µg/kg/min, p = 0.001) and the DM2 group (12.7 ± 7.4 µg/kg/min, p = 0.026).
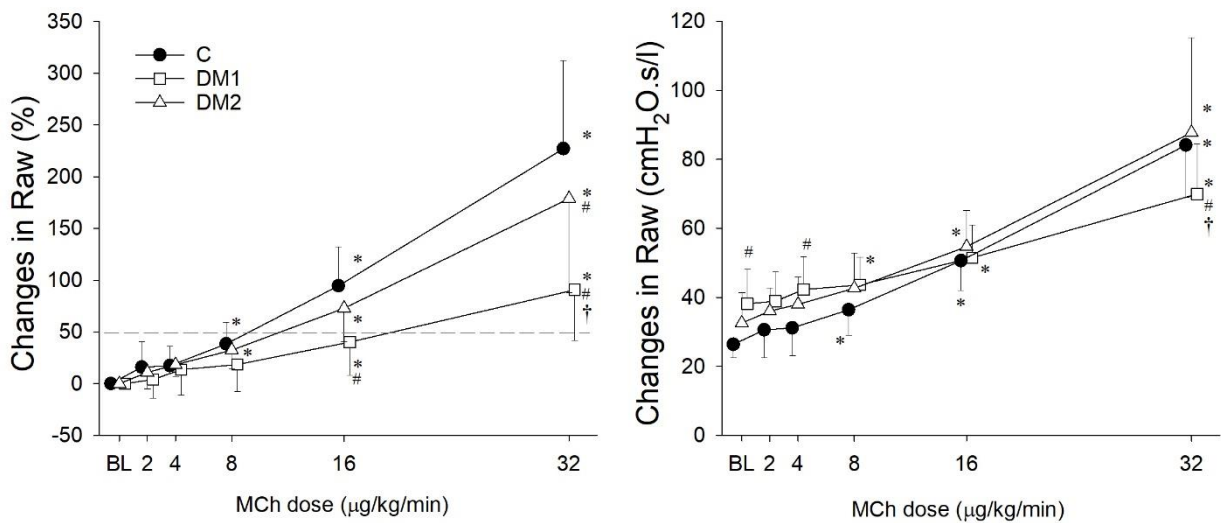
Figure 8. Airway resistance and its absolute (right) and relative (left) changes to the baseline during the *methacholine provocation tests in control rats (closed circles, C, n = 14), in rats in the type 1 diabetes (DM1, open squares, n = 13) and type 2 diabetes (DM2, open triangles, n = 14) groups. The symbols and error bars represent the mean and SD values, respectively. * p < 0.05 vs. BL within a group; # p < 0.05 vs. C within a condition; † p < 0.05 vs. DM2 within a condition*

The effect of PEEP applying on the gas exchange parameters

The parameters reflecting the gas exchange properties of the lungs are summarised in Fig 9. The rats with healthy lungs in the control group exhibited moderate values of intrapulmonary shunt (<9.3%) and physiological PaO_2/FiO_2 (>438 mmHg); these indices exhibited systematic improvements with increasing PEEP to 3 (p < 0.02) and 6 cmH_2O (p < 0.05). In the DM2 group, there was a near-significant tendency for Qs/Qt to be reduced compared to the control group at a PEEP of 6 cmH_2O (p = 0.065), whereas PaO_2/FiO_2 was reduced at a PEEP of 3 cmH_2O (p = 0.05) and tended to diminish at a PEEP of 6 cmH_2O (p = 0.069). In the DM1 group at all three PEEP levels, there were significant increases in the intrapulmonary shunt (p < 0.001) associated with markedly compromised PaO_2/FiO_2 (p < 0.001). In addition, changes in the PEEP dependence of the gas exchange parameters were observed in the DM1 group, with no monotonous improvements in Qs/Qt and PaO_2/FiO_2 with increasing PEEP.
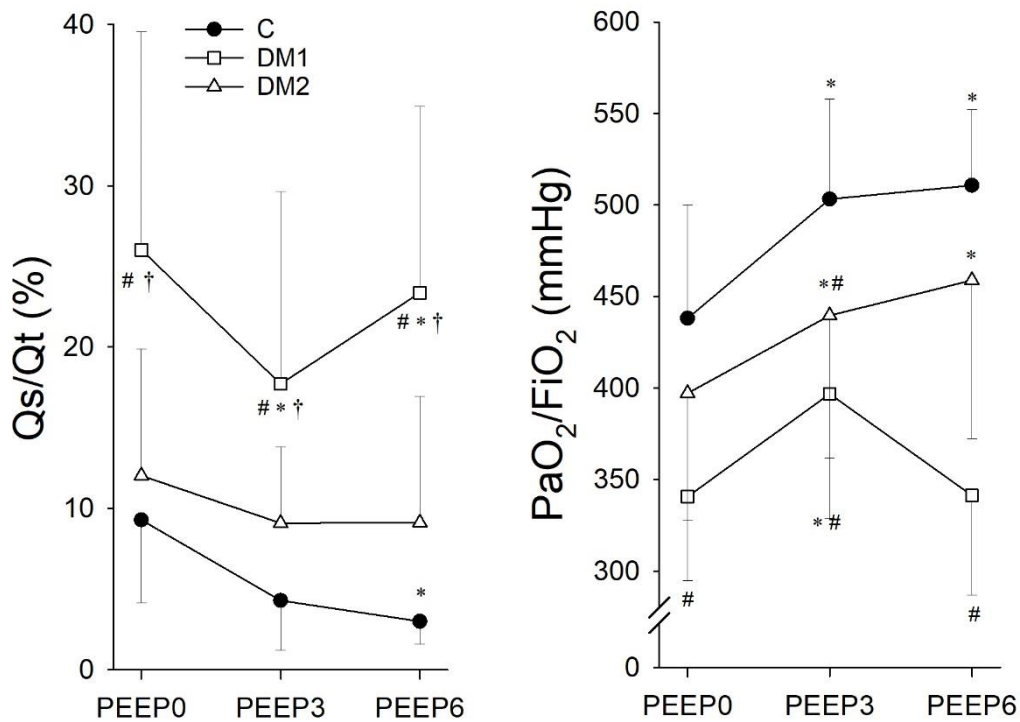
Figure 9. *Measurements obtained at positive end-expiratory pressures of 0, 3, and 6 cmH₂O (PEEP0, PEEP3, and PEEP6, respectively) in control rats (closed circles, C, n = 14) and in rats in the type 1 diabetes (DM1, open squares, n = 13) and type 2 diabetes (DM2, open triangles, n = 14) groups. The symbols and error bars represent the mean and SD values, respectively. * p < 0.05 vs. PEEP0 within a group; # p < 0.05 vs. C within a PEEP; † p < 0.05 vs. DM2 within a PEEP.*

Histological consequences

Fig 10. shows the expression of collagen in the three groups. The percentage area of collagen was significantly higher in both DM groups than in the control group ($p < 0.001$). The collagen content of the lung parenchyma was greater in the DM1 group than in the DM2 group ($p < 0.001$).
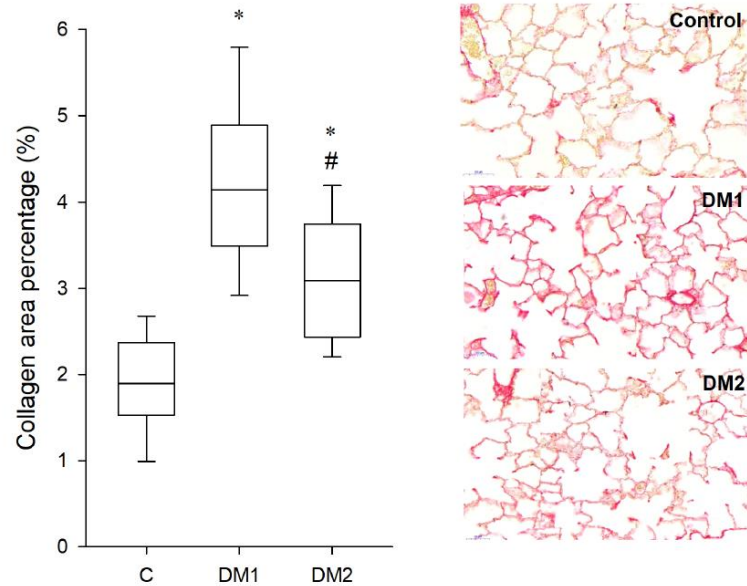
Figure 10. Collagen expression in the rat lungs. *Areas of collagen obtained from lung histology (left) and representative lung tissue sections (right) in control rats (C, n = 14) and in rats in the type 1 diabetes (DM1, n = 13) and type 2 diabetes (DM2, n = 14) groups. * p < 0.05 vs. C; # p < 0.05 vs. DM1.*

Fig 11. shows the relationship between the percentage area of collagen obtained by lung histology and the viscoelastic dissipative and elastic mechanical parameters. There were significant correlations between the histology and both tissue mechanical indices, G and H.
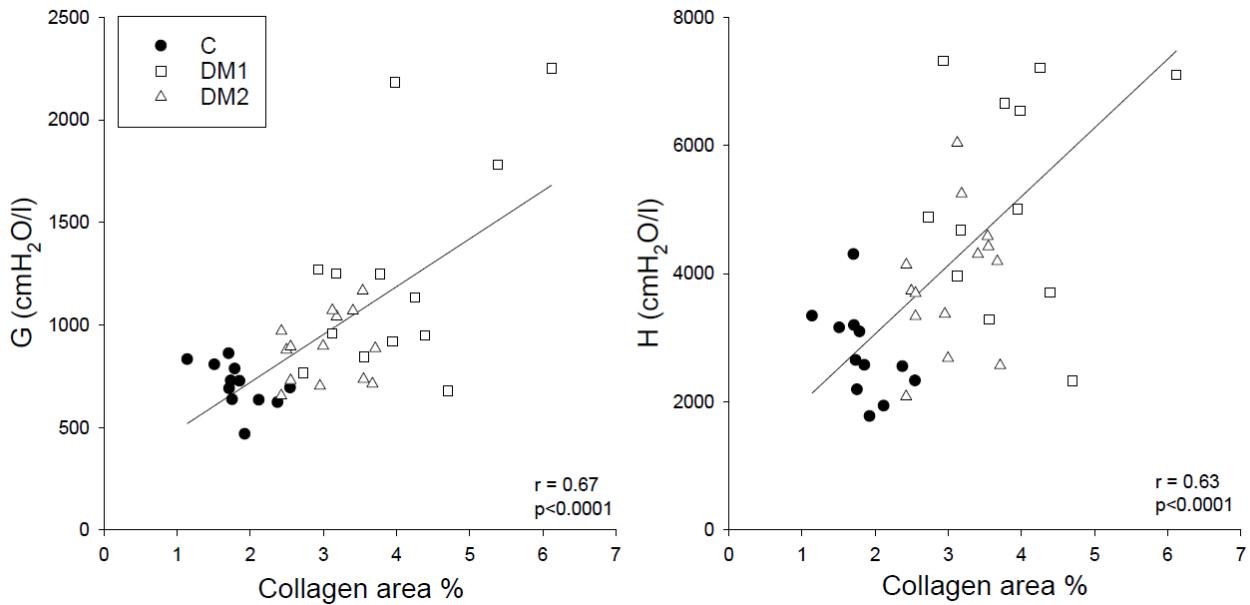
Figure 11. Correlation between the collagen and the viscoelastic parameters of the rat lungs. Correlations between the percentage areas of collagen obtained by lung histology and forced oscillation mechanical parameters for tissue damping (G) and elastance (H) in control rats (C, n = 14) and in rats in the type 1 diabetes (DM1, n = 13) and type 2 diabetes (DM2, n = 14) groups. The solid line indicates the linear regression curve.

Effects of diabetes on the cerebral integrity: results in the clinical study

Patient characteristics

Table 2 summarises the demographic, anthropometric and clinical characteristics and surgical procedures of the patients with and without T2DM. HbA1c was significantly higher in diabetic patients while there was no significant difference in the other parameters (i.e. weight, height, age or ejection fraction).

|		Group C (n=91)	Group T2DM (n=48)	p
Preoperative parameters	**Weight (kg)**	83 (79-86)	83 (77-89)	0.97
	Height (cm)	168 (166-170)	165 (163-168)	0.20
	Age (years)	65 (63-68)	68 (67-70)	0.30
	Ejection fraction (%)	60 (56-64)	56 (51-61)	0.15
	HbA1c (%)	5.6 (5.4-5.7)	7.2 (6.7-7.7)	<0.001
	Duration of T2DM (years)	-	11 (9-13)	-
Surgical procedures and diagnoses	**ARR (AAA) (n)**	1	0	1.00
	AVR (AS) (n)	28	9	0.15
	AVR (AI) (n)	1	1	1.00
	AVR+MVR (AS+MI) (n)	2	3	0.33
	AVR+CABG (AS) (n)	11	3	0.37
	AVR+CABG (AI) (n)	3	2	1.00
	MVR/P (MI) (n)	10	4	0.77
	MVR+CABG (MI+CAD) (n)	3	1	1.00
	OPCAB (CAD) (n)	31	24	0.07
	LA Myxoma (n)	1	1	1.00

Table 2: *Patient characteristics, surgical procedures and diagnoses (in parentheses) HbA1c: Hemoglobin-A1c, ARR: aortic root replacement, AAA: aortic arch reconstruction; AVR: aortic valve replacement to repair aortic stenosis (AS) or aortic insufficiency (AI); MVR/P: mitral valve replacement/plasty; CABG: coronary artery bypass grafting; MI: mitral insufficiency; LA: left atrium, CAD: coronary artery disease. Data for preoperative parameters are shown as mean and 95% confidence interval for the mean; data for surgical procedures and diagnoses are represented as number of patients.*

Serum glucose level, $CrSO_2$ and parameters determining tissue oxygen balance obtained before anaesthesia induction are demonstrated on Table 3. The serum glucose level was higher and the $CrSO_2$ values were lower in the T2DM patients as compared to the control patients. Evidence for a difference in parameters determining the oxygen supply was only observed in haemoglobin concentration and CaO_2. Response entropy, state entropy and oesophageal temperature did not differ between the protocol groups.

	Group C (n=91)	Group T2DM (n=48)	p
Glucose (mmol/L)	5.9 (5.7-6.0)	8.04 (7.2-8.9)	<0.001
$CrSO_2$ (%)	68 (66-69)	60 (58-63)	<0.001
MAP (mmHg)	88 (86-90)	86 (83-90)	0.29
CaO_2 (ml/dl)	17.0 (16.4-17.5)	16.0 (15.2-16.7)	0.034
Haemoglobin (g/dl)	13.0 (12.7-13.5)	12.4 (11.9-13)	0.043
PaO_2 (mmHg)	77.09 (71.70-82.48)	72.29 (69.11-75.46)	0.13
pHa	7.412 (7.408-7.417)	7.408 (7.396-7.420)	0.86
$PaCO_2$ (mmHg)	38.27 (37.27-39.26)	37.88 (36.46-39.31)	0.66
RE	90 (83-96)	92 (86-97)	0.394
SE	86 (79-92)	91 (84-97)	0.33
Te (°C)	36.5 (36.2-36.7)	36.7 (36.2-37.0)	0.6
CPB duration (min)	83 (74-92)	89 (69-109)	0.625

Table 3: Intraoperative parameters before anaesthesia induction. The serum glucose level and initial cerebral tissue oxygen saturation ($CrSO_2$) with parameters determining tissue oxygen balance. MAP: mean arterial pressure; CaO_2: arterial oxygen content; PaO_2: arterial partial pressure of oxygen; $PaCO_2$: arterial partial pressure of CO_2; RE: response entropy; SE: state entropy, Te: oesophageal temperature, CPB: cardiopulmonary bypass. Data are shown as mean and 95% confidence interval for the mean

Effects of T2DM on central venous and cerebral oxygen saturation during CPB and OPCAB procedures

Oxygen saturation in central venous blood ($ScvO_2$), in cerebral tissue ($CrSO_2$) and their difference expressed as a saturation gap (gSO_2), are presented in Fig 12 for the patients underwent cardiac surgery with (top) or without (bottom) CPB. No significant difference was observed in $ScvO_2$ between patients with and without T2DM at any protocol stage. Conversely, $CrSO_2$ was significantly lower in the T2DM-CPB and T2DM-OPCAB groups than in the corresponding controls ($p<0.001$ for both), and this difference endured in all phases of the surgery. This result was reflected in significant differences in gSO_2 between patients with and without T2DM in the CPB and OPCAB patients ($p<0.001$ for both). During the surgical procedure, prominent and significant increases in $ScvO_2$ ($p<0.001$) with smaller but statistically significant decreases in $CrSO_2$ ($p<0.05$) were observed at the beginning of CPB, resulting in marked elevations in gSO_2 ($p<0.001$). In both CPB groups, the $ScvO_2$ and gSO_2 reversed by the end of CPB, and these parameters decreased below their initial levels in C-CPB patients ($p<0.005$). No significant intraoperative changes were observed in the oxygen saturation parameters in the OPCAB patients.

Effects of T2DM on clinical parameters affecting cerebral oxygen supply and demand

Main clinical parameters characterizing tissue oxygen balance obtained at different stages of the protocol are summarised in Figs 13-16. Between-group differences were observed only in the CaO_2 before the surgical procedure (Fig 13, $p<0.05$) in the blood glucose levels throughout the surgery (Fig 16, $p<0.05$) and in the arterial oxygen saturation $CrSO_2$ differences (Fig 13 $p<0.05$). Considerable within-group intraoperative changes were observed primarily during the CPB procedure. The onset of CPB was associated with small but significant decreases in core body temperature in both T2DM-CPB and C-CPB patients (Fig 15, $p<0.05$), which subsequently returned to the initial value by the end of the surgery. Furthermore, MAP and CaO_2 decreased significantly in both groups of patients when CPB was established (Fig 13, $p<0.05$), and returned to their initial values following chest closure. RE and SE decreased significantly after anaesthesia induction in all groups of patients with no difference between patients with and without T2DM (Fig 15).
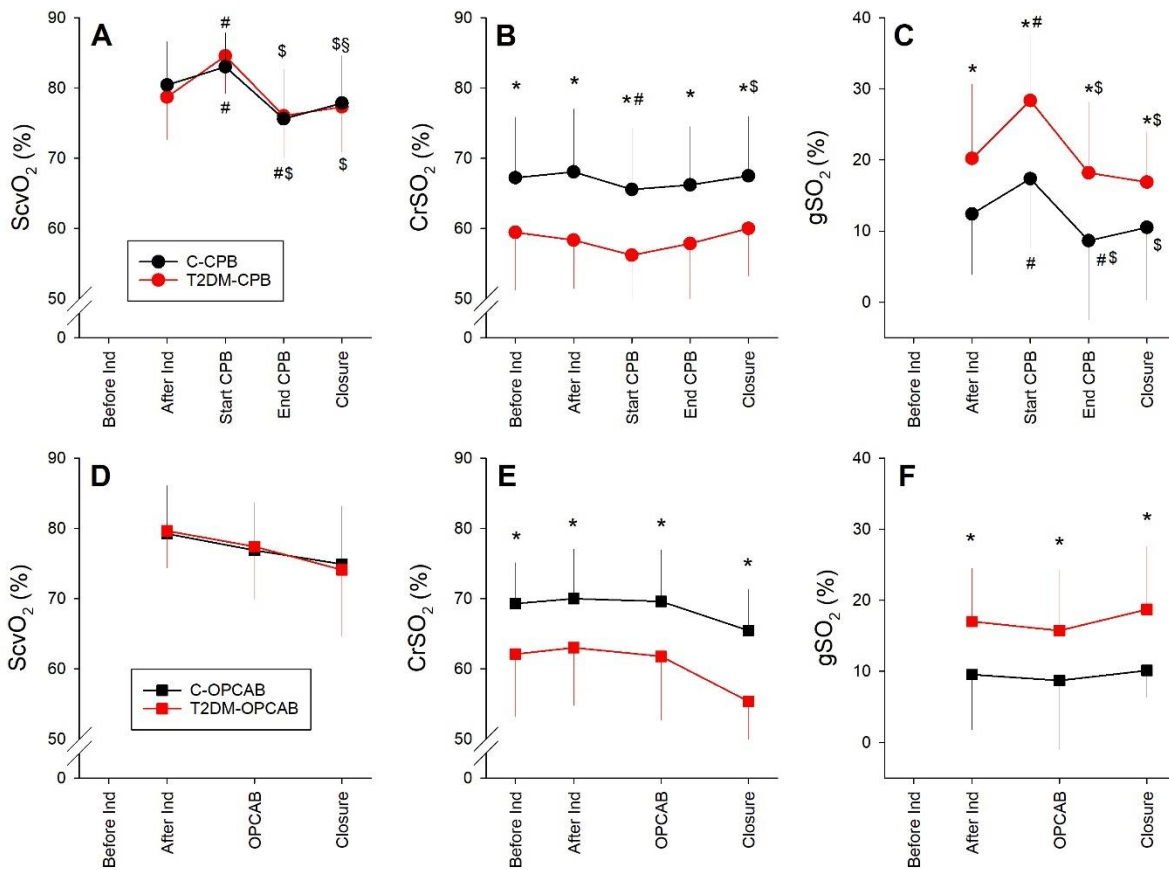
Figure 12. The central venous oxygen saturation (ScvO₂, panels A and D), the cerebral oxygen saturation (CrSO₂, panels B and E) and the differences between these indices (gSO₂, panels C and F) according to the protocol stages in patients with (red symbols) and without T2DM (black symbols) who underwent CPB (top panels) or OPCAB procedures (bottom panels). Error bars represent the following: SD. *: p<0.001 between the protocol groups within a stage, #: p<0.05 vs. stage "After Ind.", $: p<0.05 vs. condition "Start CPB", §: p<0.05 vs. condition "End CPB" within a group

Figure 13. Intraoperative changes in the parameters determining cerebral-tissue oxygen supply *in patients with (**n=48, red symbols**) and without (**n=91, black symbols**) diabetes mellitus. CPB procedures on the top, OPCAB procedures are on the bottom panels. **MAP:** mean arterial pressure, **CaO₂:** arterial oxygen content, **pHa**: arterial pH. *: p<0.05 control vs. T2DM, +: p<0.05 vs. before induction, #: p<0.05 vs. after induction, $: p<0.05 vs. start CPB or OPCAB, §: p<0.05 vs. end CPB.*

Figure 14. Intraoperative changes in the oxygenation index (PaO₂/FiO₂), arterial oxygen saturation (SaO₂) and the differences between arterial and central venous (SaO₂-ScvO₂) and cerebral-regional saturation (SaO₂-rSO₂) (n=48, red symbols) and without (n=91, black symbols) diabetes mellitus. CPB procedures on the top, OPCAB procedures are on the bottom panels. *: p<0.05 control vs. T2DM, +: p<0.05 vs. before induction, #: p<0.05 vs. after induction, \$: p<0.05 vs. start CPB or OPCAB
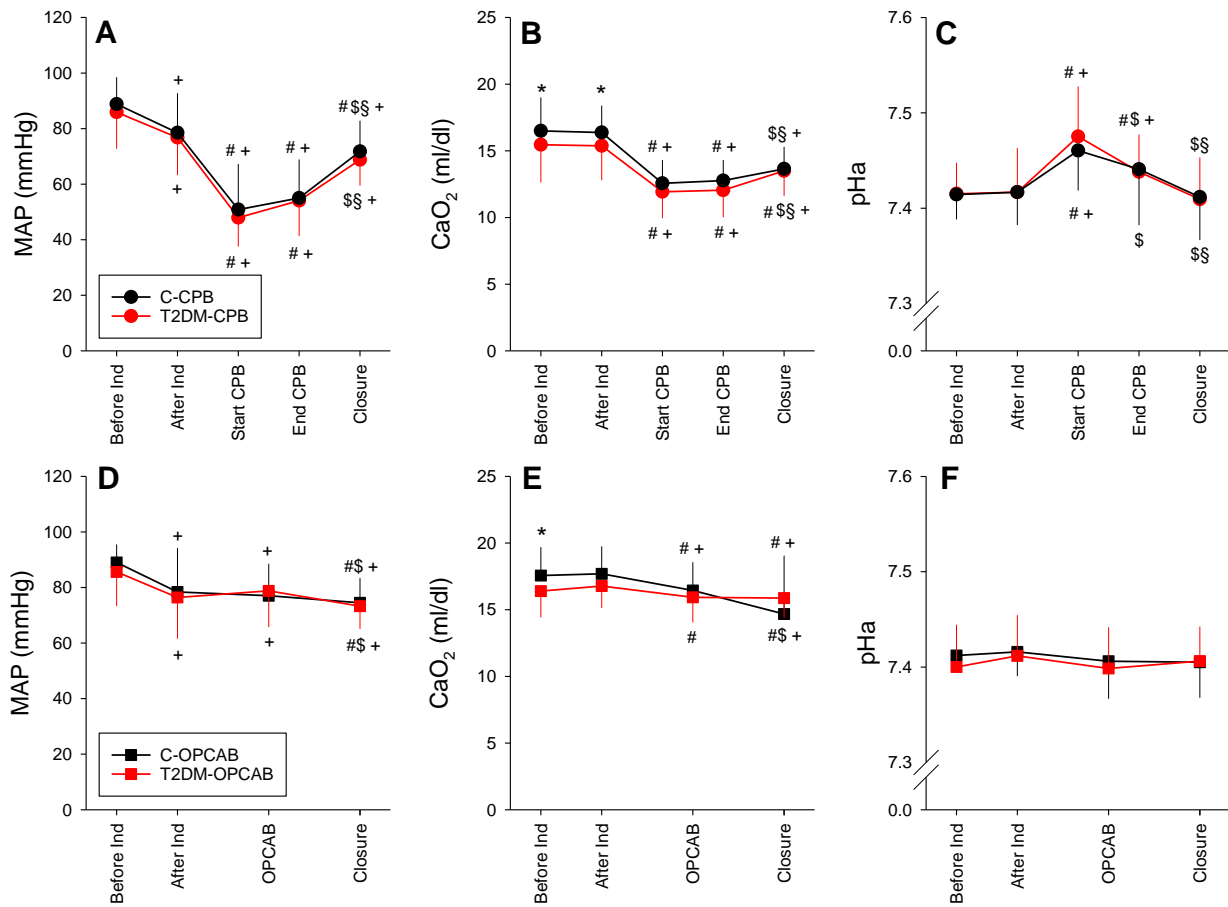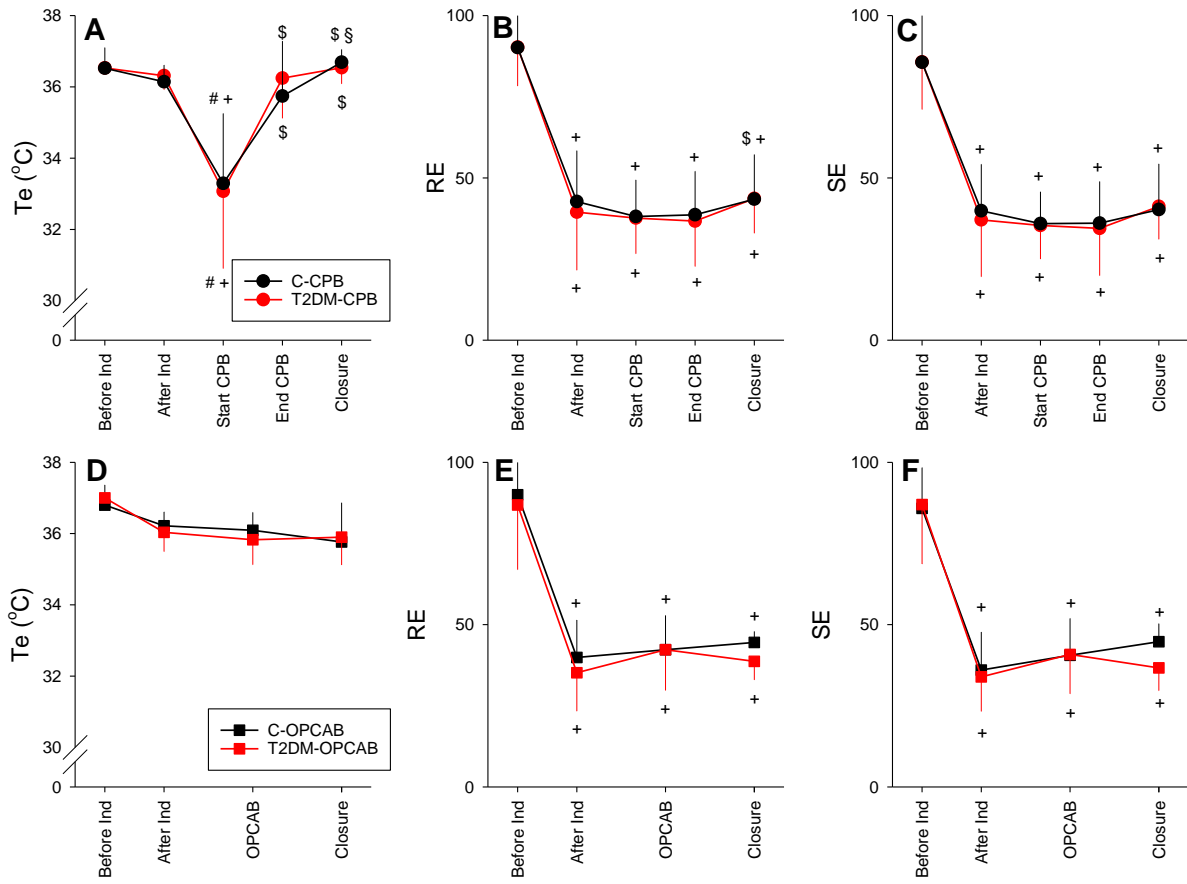
Figure 15. Intraoperative changes in the parameters determining cerebral-tissue oxygen demand *in patients with (**n=48, red symbols**) and without (**n=91, black symbols**) diabetes mellitus. CPB procedures on the top, OPCAB procedures are on the bottom panels.* ***Te:*** *oesophageal temperature,* ***RE:*** *Response Entropy,* ***SE:*** *State Entropy. +: $p<0.05$ vs. before induction, #: $p<0.05$ vs. after induction, $: $p<0.05$ vs. start CPB or OPCAB, §: $p<0.05$ vs. end CPB*
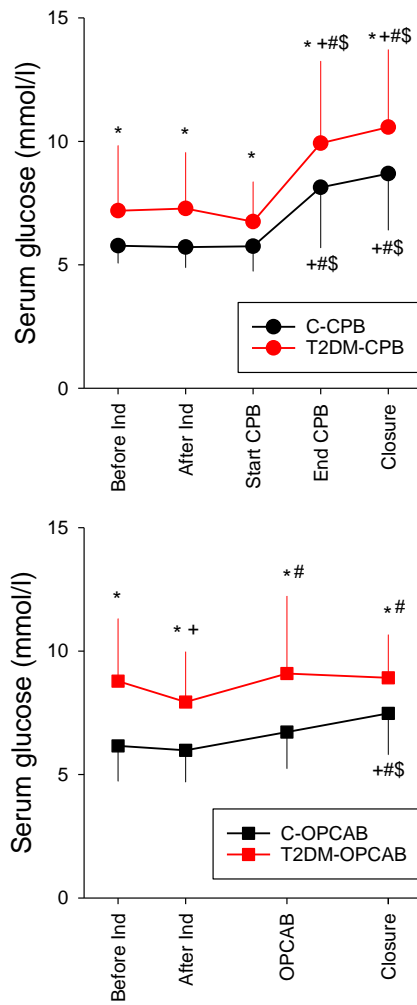
Figure 16. Intraoperative changes in serum glucose levels in patients with (**n=48, red symbols**) and without (**n=91, black symbols**) diabetes mellitus. CPB procedures on the top, OPCAB procedures are on the bottom panels. *: $p<0.05$ control vs. T2DM, +: $p<0.05$ vs. before induction, #: $p<0.05$ vs. after induction, $: $p<0.05$ vs. start CPB or OPCAB
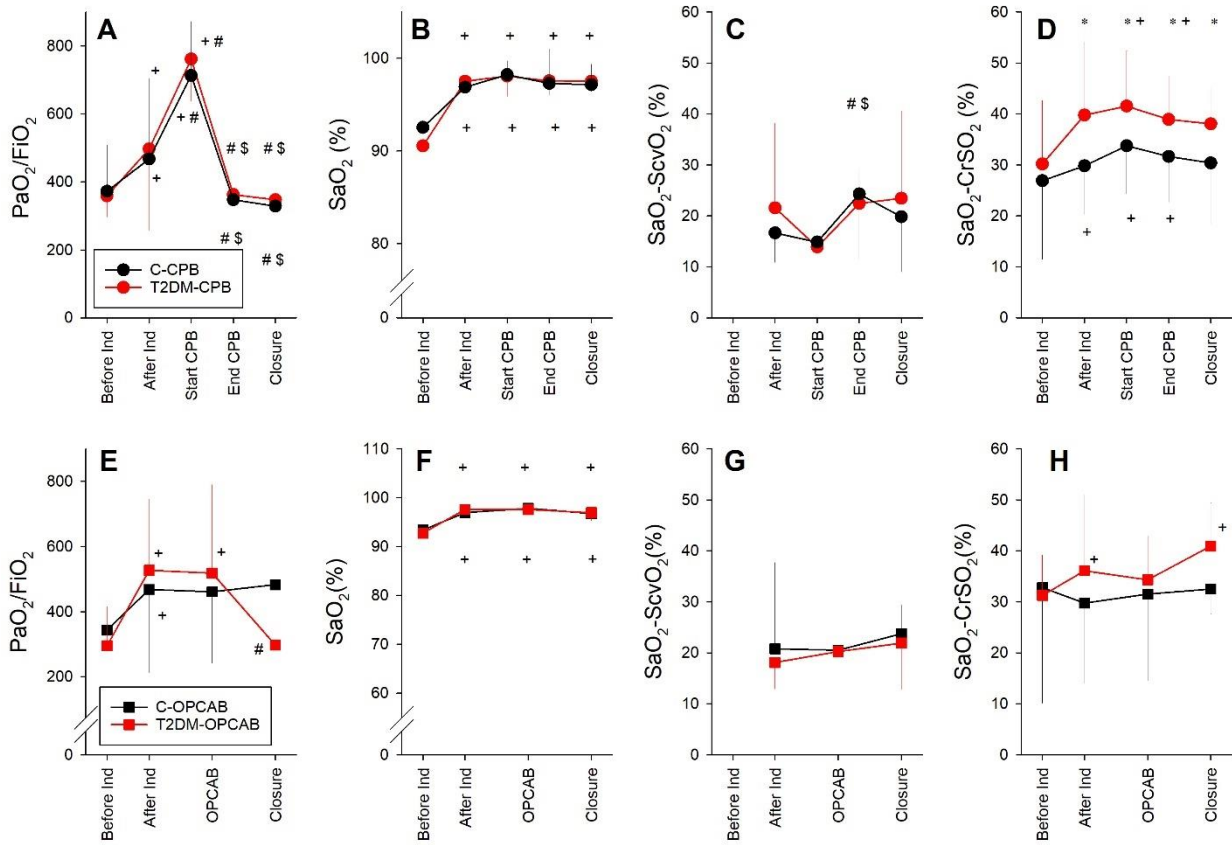
Relationship between central venous and cerebral oxygen saturation: effects of T2DM

The relationship between central venous and cerebral oxygen saturation obtained after anaesthesia induction prior to the surgery for control and T2DM patients is illustrated in Fig 17. Significant correlation was observed between $ScvO_2$ and $CrSO_2$ in the control group. In contrast, no significant correlation was found between these global and regional oxygen saturation parameters in patients with T2DM.
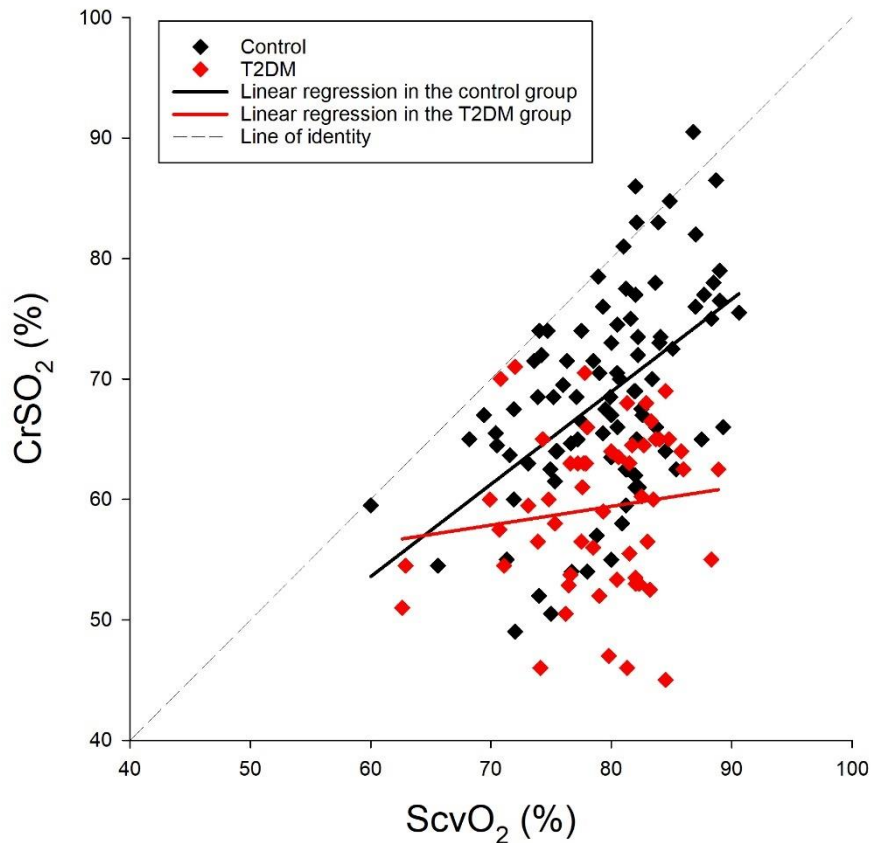
Figure 17. Correlation between cerebral oxygen saturation (rSO_2) and central venous oxygen saturation ($ScvO_2$) after the induction of anaesthesia in each patient. Linear regression in the T2DM group (p=0.34, r=0.13), Linear regression in the control group (p<0.0001, r=0.52).

DISCUSSION

In diabetes, detrimental changes on molecular, cell and tissue level lead to multiorgan damage. While the effects of diabetes are studied excessively, there are still lack of knowledge how diabetes affects distinct organs. Thus, we investigated the impact of diabetes on two vital organs, the lung and the brain. Chronic hyperglycaemia lead to pathophysiological intracellular pathway activation resulting in *i.e.* ROS overproduction, PKC-activation, TGF-β overexpression, glycation (Fig 1.). The resulted IC and EC protein, endothelial and epithelial damage manifest in vascular and bronchial smooth muscle cell and connective tissue dysfunction, leading to deteriorations both in the respiratory system and in the brain. The respiratory consequences of DM were studied in well-established rodent models, which allowed the use of complex measurement techniques without the influence of other potentially confounding factors (i.e. age, the onset of the disease, or comorbidities). The cerebral effects were investigated in a patient population in which the presence of diabetes is more frequent and susceptible to further organ damage. Since diabetes affects approximately one third of the patients undergoing cardiac surgery, a surrogate of the tissue oxygenation, the $CrSO_2$ was measured before and during cardiac surgery to elucidate the effect of diabetes on cerebral tissue oxygenation.

Effect of diabetes on the respiratory system: experimental study

The characterization of the pulmonary effects of DM in this study revealed detrimental changes in airway function, viscoelastic tissue mechanics, gas exchange, and collagen expression in the lung, with more severe manifestations in the rat model of type 1 DM than in that for type 2 DM. The increase in the basal airway tone with DM was associated with compromised dissipative and elastic tissue mechanics. The model of type 1 DM also showed diminished airway responsiveness to an exogenous cholinergic stimulus. These adverse mechanical and functional changes were accompanied by an increased intrapulmonary shunt and impaired PaO_2/FiO_2. Increasing the lung volume had a beneficial effect on the lung mechanics in both diabetic groups, whereas it had no benefit on gas exchange.

This study used well-established models to induce type 1 and 2 DM [101-106]. Type 1 DM was induced by a single high dose of STZ to cause the destruction of the pancreas, whereas type 2 DM was induced by a low dose of STZ to cause diffuse degeneration of the pancreatic cells, combined with a high-fat diet. As a result of these treatments, the blood glucose levels in both DM groups were markedly higher after 12 weeks than those of the control group. The body weight of the type 1 DM group rats was reduced, which can be explained by insulin deficiency [117, 118]. As with

other chronic complications of DM, the pulmonary complications would be expected to manifest in the late stage of the condition [21]. For this reason, a 12-week period was allowed for the animals to develop lung dysfunction. This long period with markedly elevated serum glucose levels allowed the development of adverse pulmonary symptoms without a fatal outcome.

Changes in the mechanical properties of the respiratory system

Forced oscillatory assessment of airway mechanics showed that DM caused a deterioration of basal Raw, with more severe changes occurring in the type 1 DM model rats (Fig 8 PEEP0). As these changes were also apparent in the specific airway resistance values (Table 1) of both DM groups, the differences in lung sise cannot solely be accounted for by the compromised airway mechanics. Instead, these pathological changes in the airways may be explained by the decreased vagal tone [119], excessive mucus production [120], low-grade chronic inflammation [121], activation of inflammatory pathways [122], or bronchial smooth muscle cell proliferation [123, 124]. The present study's finding of increased airway tone in the DM rat models is in qualitative agreement with the results of previous studies that assessed airway resistance in DM [45, 125], providing supporting evidence for the potential development of chronic airway obstruction in patients with DM.

The effects of DM on the mechanical properties of the lung tissue has been studied in an *ex-vivo* experiment, and the results were limited to assess the elastic behaviour of the lung parenchyma [52] However, dissipative properties of the lung tissue play an important role in determining the physiological lung mechanics and the changes of this component is characteristic in various lung diseases [126]. In the present study using an *in-vivo* setting, significant deteriorations were observed in the viscoelastic mechanical parameters of the respiratory tissues in both groups of diabetic rats (Fig 8), and this adverse change affected both the dissipative and elastic properties. These differences compared to the control group remained after normalization of the values to the FRC (Table 1), indicating that intrinsic changes to the dissipative and elastic properties of the respiratory tissues can be anticipated. Collagen is the main determinant of overall lung tissue viscoelasticity [127, 128]. In the present study, the volume of collagen increased in the DM models, in agreement with results reported for patients with DM [129] (Fig 11). There were significant correlations between the histological and mechanical findings (Fig 12), which suggested that the overexpression of collagen may be a primary cause of the compromised tissue damping and elastance observed in DM. The underlying pathophysiological mechanisms responsible for this extracellular matrix remodelling may be related to the activation of pathological pathways that contribute to the formation of AGEs, which also stimulate the

production of extracellular matrix components, including collagens, thereby affecting the interactions of the extracellular matrix [13].

Effect of PEEP on respiratory function

Increasing numbers of patients with DM require surgical procedures that involve mechanical ventilation, which has increased the burden on healthcare providers [130, 131]. There is, therefore, a need for awareness that adequate mechanical ventilation should be provided for these patients. Open lung strategies require the application of an appropriate PEEP; however, the impact of different levels of PEEP on respiratory function in DM has not been clarified. Our findings demonstrated that the between-group differences in the airway resistance and in the tissue mechanical parameters representing viscoelastic dissipation and elastance disappeared at a moderately elevated PEEP (6 cmH$_2$O; Fig 7). The excessive PEEP dependence of the respiratory mechanical parameters was consistent with the diminished surfactant function reported previously in models of DM [36, 37]. It suggests that applying PEEP can have a beneficial effect on respiratory mechanics in this metabolic disease. The mechanical improvements were reflected in the decreased intrapulmonary shunt and increased PaO$_2$/FiO$_2$ in the DM rats when a PEEP of 3 cmH$_2$O (Fig 10) was applied. Nevertheless, substantial differences remained even with elevated PEEP in both groups of DM rats; this can be attributed to the persistent alveolar-capillary barrier damage observed in DM [44, 129, 132]. The type-II pneumocyte and surfactant layer damage [36, 37] along with the low-grade inflammation [44] observed in DM can contribute to the alveolo-capillary dysfunction. Noticeably, there was recurrent deterioration of PaO$_2$/FiO$_2$ and Qs/Qt in the type 1 DM rats at a PEEP of 6 cmH$_2$O. This group would be expected to develop the well-established adverse pulmonary vascular consequences of hyperglycaemia [133]. Accordingly, formation of AGEs as detailed above contributes to a proliferation of pulmonary endothelial and vascular smooth muscle cells and thicker basal lamina [134], which may have resulted in the intra-acinar and alveolar arterioles becoming prone to collapse when the PEEP exerted an external mechanical load on the capillary network.

Changes in airway response to exogenous stimuli

An important physiological feature of airways is the adaptation of their caliber in response to exogenous stimuli. The results for the type 1 DM group demonstrated diminished airway responsiveness to MCh, which indicated that the adaptation ability of the bronchomotor tone had been severely compromised. Pathophysiological mechanisms that may have been involved in the decreased airway responsiveness include compromised vagal tone development due to autonomic diabetic neuropathy [119, 135], smooth muscle cell dysfunction [136], and/or epithelial damage

[29]. Hyperinsulinemia, insulin resistance and hyperglycemia can lead to hyperproliferation and phenotype changing of the airway and bronchial smooth muscle cells and induce tracheal wall thickening [123, 124]. The smooth muscle cell damage might occur due to various factors, for instance disturbances in the nitric oxide synthesis [29], TGF-β and Rho-associated protein kinase pathway activation [32, 137, 138]. Nonetheless, conflicting results have been reported for the effects of DM on airway responsiveness. The findings of the present study are consistent with earlier findings of a reduction in the bronchial response to cholinergic stimuli in DM [29, 47, 139]. Previous reports of no change in airway responsiveness [46, 136, 140] or the development of airway hyperresponsiveness [32, 33, 141] may be explained by the insensitivity of the methods to assess airway function [136], the lack of airway innervation [32, 33, 140], or the involvement of confounding factors, such as, smoking, genetic differences and/or phenotype, and the duration of DM [46, 141]. Furthermore, in previous clinical studies, diabetes was often associated with comorbidities affecting the respiratory system, which may cause variation in the manifested pulmonary effects, and can contribute to the discordant results in the literature.

Effect of diabetes on the cerebral integrity: clinical study

Significant reduction of brain tissue oxygen saturation was obtained in the present study in T2DM patients. Since this finding was not reflected in the central venous oxygen saturation, the gap between $ScvO_2$ and $CrSO_2$ widened significantly and the relationship between these two values became uncoupled in patients with diabetes. In the T2DM patient, the oxygen saturation gap remained elevated throughout the cardiac surgery procedure.

Differences in the initial parameters between patients with and without diabetes

The lower initial $CrSO_2$ (Fig 12, B and E) and the associated widening of gSO_2 (Fig 12, C and F) in patients with T2DM cannot be attributed to differences in demographic, anthropometric and clinical characteristics between the two groups (Tables 2 and 3). In both groups of patients, the oxygen demand of the cerebral cortex was expected to be in a uniformly low range throughout the surgery, as suggested by the therapeutic entropy levels (Fig 15). While the glucose levels differed between normal and diabetic patients (Table 3 and Fig 16), the uniformly negligible extinction coefficient in the observed wavelength [142] does not bias our findings. The higher glucose concentration of the T2DM group can lead to different light scattering in tissue [143], however the magnitude of this methodological artefact is could not be great enough to result in such a significant difference in the two study groups. Therefore, this phenomenon could not explain our findings on the $CrSO_2$ difference between the diabetic and control groups. The presence of anaemia and lower CaO_2 in the T2DM patients (Table 3) may contribute to the differences in $CrSO_2$

between control and diabetic patients. However, $ScvO_2$ did not differ between the protocol groups (Fig 12), suggesting sufficient oxygen supply in all patients under general anaesthesia with muscle relaxation when the oxygen demand of the paralyzed skeletal muscle decreases markedly. Accordingly, the diminished overall oxygen extraction can be supplied both in patients with normal or compromised microcirculation (such as T2DM). Moreover, the widened gap in diabetic patients remains after CPB despite the lack of difference in CaO_2 and MAP between diabetic and non-diabetic patients. Most probably, the compromised $CrSO_2$ can rather be explained by the adverse cerebrovascular consequences of T2DM. The pathologic metabolic milieu is characterised by hyperglycaemia, insulin resistance and elevated level of free fatty acids [144]. Interruption of the vasodilatory insulin signalling pathway diminishes endothelial nitric oxide (NO) synthesis [145]. Endothelial NO production is further compromised by the advanced glycation end-products [145] and by the increased inactivation of NO by oxidative stress [145]. The reduced NO-mediated endothelium-dependent vasodilation increases the vascular tone. The elevated arterial tone and/or vascular remodelling facilitated by these mechanisms are associated with low-grade inflammatory, prothrombotic proliferative processes, resulting in atherosclerotic plaque formation [146]. All these mechanisms converge to an impaired microcirculation [8], which may be reflected in impaired cerebral-tissue oxygen saturation.

The few previous results available for anaesthetised patients measured before surgical intervention revealed somewhat lower cerebral oxygen saturation in diabetic than non-diabetic patients [99, 147, 148], or failed to demonstrate an effect of diabetes on this outcome [149]. The discrepancies between these earlier results and the current finding may be attributed to the relatively small number of patients involved in the previous studies. Considering the substantial inter-individual variability in our $CrSO_2$ data obtained in diabetic patients (Fig 12), the statistical power may not have been robust enough to reach a conclusion with confidence in the previous studies. All these previous studies applied jugular venous bulb oximetry to assess cerebral oxygen saturation, which reflects the oxygen status of the entire brain, whereas NIRS utilised in the present study focuses on the cortex. Since both the blood flow and oxygen demand is higher in the cortex than in the white matter [98], microvascular dysfunction and remodelling may be more apparent in the cortical region. The sole previous study where NIRS data were reported for a diabetic subpopulation was part of a preoperative assessment without evaluating changes in the intraoperative period [150]. In this study, diabetes was associated with lower baseline $CrSO_2$ in vascular surgery patients; however, patients undergoing cardiac surgery procedures exhibited no difference preoperatively. Nevertheless, the high ratio of smokers and inclusion of aged patients in this previous study may have blunted the distinct effects of diabetes on the measured outcomes.

Intraoperative changes

Remarkable intraoperative changes were observed in $ScvO_2$, $CrSO_2$ and gSO_2 at the beginning of CPB (Fig 12, top panel). The increases in $ScvO_2$ can be attributed to a decreased core temperature (Fig 15) and subsequent decrease in the systemic oxygen demand [151]. The concomitant slight, but significant, decrease in $CrSO_2$ in the diabetic patients should be interpreted in terms of a decreased MAP and haemoglobin concentration associated with an elevation in arterial pH (Fig 14) [152]. The opposite changes in $ScvO_2$ and $CrSO_2$ after the onset of CPB are reflected in the striking elevations in gSO_2 (Fig 11 C). It is of note that in diabetic patients the gSO_2 may rise to a value threefold greater than physiologically normal (i.e. from around 10 to around 30 %, Fig 12 C). The compromised $CrSO_2$ observed in the present study may be responsible for the increases in postoperative adverse neurocognitive outcomes and stroke in T2DM patients [92-95]. In contrast with the CPB patients, no intraoperative changes in oxygen saturation indices were detected in the patients with OPCAB procedures (Fig 12, bottom panel). This more stable pattern of cerebral-tissue oxygen saturation may explain the lower incidence of postoperative stroke [94, 153] and cognitive dysfunction [154] after cardiac surgery with OPCAB.

The brain has high oxygen demand as well as low hypoxic tolerance and the regulation of cerebrovascular circulation is correspondingly complex [155]. Therefore, the oxygen saturation of this organ can distinctly differ from the rest of the systemic circulation. NIRS offers a simple, non-invasive, real-time monitoring tool to quantify the oxygen status of brain tissue. Hence, this technique has a great potential to reveal disturbances in the regional oxygen saturation promptly, with a particular advantage of assessing cerebral tissue oxygen saturation in the perioperative period. In non-diabetic patients, there is a significant difference between global and cerebral-tissue oxygen saturations, although they exhibit significant correlations (Fig 17). Nevertheless, there is a scatter in this relationship due to recognised interindividual variability in even in the control patients [156, 157]. Nevertheless, the associations between these regional and global oxygenation indices suggest the possibility to predict of the brain oxygen status from the $ScvO_2$ value when the cerebral circulation is intact. Conversely, our results also demonstrate that in addition to the gap between $ScvO_2$ and $CrSO_2$, these parameters became uncoupled in diabetic patients (Fig 17). The lack of a clear relationship between these indices impedes the assessment of cerebral-oxygen saturation from $ScvO_2$ in the T2DM population. Accordingly, our findings demonstrate the particular monitoring value of NIRS in the presence of a disease affecting cerebral microcirculation. These considerations may contribute to the clarification of the monitoring value of NIRS in a critically ill population, which is currently under debate [158-161].

LIMITATIONS OF THE STUDIES

Several methodological aspects of the present studies warrant consideration. As well-established models were adapted in the experimental study to produce the most important features of DM, including hyperglycaemia and insulin deficiency, verification of the effectiveness of the STZ treatments was limited to evaluating serum glucose levels; a detailed characterization of the resulting metabolic profile would go beyond the focus of the present investigation. The models of type 1 and type 2 DM differed only in the dose of STZ and the diet regimen. The high dose of STZ administered to the rats in the type 1 DM group was likely to destroy most of the pancreatic β-cells, whereas less severe β-cell destruction in the type 2 DM group was complemented by a high-fat diet to induce a combination of impaired insulin production and peripheral insulin resistance [102, 118]. The difference in body weight between the groups suggested marked differences in their metabolic status; however, the respiratory consequences were analogous in the two DM groups, with symptoms differing only in severity. The animal study was designed to focus primarily on the changes in the mechanical properties of the respiratory system in diabetes. However, there are plethora of diagnostic tools to characterise pulmonary dysfunction both at on organ and at cellular levels. Analyses of bronchoalveolar lavage fluid to assess altered surfactant function, or quantitative collagen and smooth muscle cell assays by using immunohistochemistry methods would give further insights into the underlying mechanisms; these methods may be subjects of forthcoming investigations.

A methodological aspect of the clinical study is related to the general limitations of the NIRS in the accurate assessment of cerebral oxygenation, such as lack of established baseline values, possible contamination by scalp tissue, localised reading and the assumption of fixed arterial-venous blood ratio of the tissue [158, 162]. The INVOS-monitor is considered in the first place as a trend monitor. However, several studies reporting the absolute values of the $CrSO_2$ [163, 164], despite the high interindividual variability. In our study, this variability existed, but the high number of involved patients enabled to observe a statistically significant difference in the two groups. Another methodological aspect concerns the interindividual variability in the cardiac surgery patients. However, the groups of the patients with and without T2DM did not differ in anthropometric parameters, diagnoses or surgical procedures, and the comorbidities with potential biasing effect on cerebral circulation were excluded. This study focused on the intraoperative changes of tissue oxygenation, further studies are required to follow-up potential differences in the clinical outcomes (e.g. stroke or neurocognitive dysfunction) between normal and T2DM patients.

SUMMARY AND CONCLUSION

The studies included the present thesis emphasise the diabetic consequences both on the respiratory and cerebral function and contribute to better understanding the effect of diabetes on these organs. We demonstrated that diabetes deteriorates respiratory function, but PEEP elevation is beneficial for the mechanical properties, whereas it was not advantageous on the gas exchange parameters and oxygenation. As a consequence of the diabetic pathophysiological milieu, the cerebral regional oxygen saturation was compromised and the gap between $CrSO_2$ and $ScvO_2$ widened suggesting that the cerebral autoregulation is impaired. These deteriorations originate from the complex yet common pathophysiological changes in diabetes.

As a summary of the experimental study, distinct measurements of airway and respiratory tissue viscoelastic parameters in models of T1DM and T2DM showed evidence of detrimental changes in both compartments. The decline in airway function was reflected in elevated airway resistance and abnormal adaptation of the airways to exogenous constrictor stimuli. Lung tissue remodelling was manifested in compromised viscoelastic tissue mechanics, which affected dissipative and elastic properties, and the concurrent overexpression of collagen fibres in the extracellular matrix. These detrimental mechanical defects were overcome by applying PEEP, which demonstrated alveolar collapsibility in DM. However, even with the application of PEEP, gas exchange parameters remained compromised in the models of type 1 and type 2 DM, even deteriorated further in the type 1 DM model, indicating alveolo-capillary dysfunction.

Damages in the cerebral function are well known, however there were no study previously comparing the rSO_2 between diabetic and control in anaesthetised patients during cardiac surgery. Furthermore, the relationship between the cerebral regional and the central venous saturation was not clarified earlier. The clinical study included in the present thesis demonstrated that diabetes mellitus worsens the oxygen saturation of the cerebral tissue and uncouples indices reflecting regional cortical and global central venous oxygenation. Consequently, disturbances in the cortical oxygen saturation in diabetic patients become unpredictable from the well-established global clinical parameter of central venous oxygen saturation. Thus, diabetic patients may benefit from the continuous intraoperative measurement of $CrSO_2$ to optimise tissue oxygenation with adjusting cerebral perfusion pressure, arterial oxygen content and/or avoiding alkalosis.

In conclusion, the studies included in the present thesis are contributing to better understanding the detrimental effects of diabetes mellitus. Thus, the results foster better clinical practice contributing advanced therapeutic intervention, and safer perioperative patient care.

ACKNOWLEDGMENTS

First, I would like to express my gratitude to my supervisors. I would like to thank to Professor Barna Babik to introducing me in research and guiding me since the third year of medical school. I greatly appreciate his mentoring, and trust he placed in me. I would like to thank to Professor Ferenc Petak for all the support he provided me during these years. I could not be able to perform my research projects without his advice, help and guidance. I am grateful for sharing their immense knowledge and expertise.

I am grateful to Professor Walid Habre for the opportunity joining his lab and learning new techniques. I am thankful for his support and I truly appreciate his work; he had a great influence on me. I would like to thank Professor Ferenc Bari for allowing me to accomplish my research in the Department of Medical Physics and Informatics. I would like to thank to all the members of the Department of Medical Physics and Informatics for their kindness. I would like to thank to József Tolnai for helping me to carry out measurements and data analysis and to Orsolya Ivánkovitsné Kiss for her technical help and guidance in the animal experiments. I am grateful to the staff of the Department of Cardiac Surgery and Anaesthesiology and Intensive therapy at the University of Szeged for their contribution to the clinical study. I would like to thank to Ádám Balogh and Gergely Fodor for helping me since med school. I am thankful for Álmos Schranc for his enormous help carrying out the experiment. I thank to André Dos Santos Rocha for being the best lab mate and a good friend. And lastly, my biggest appreciation to my husband Miklós Kassai and all my family and friends for their support.

REFERENCES

1.   Organization WH: **Global report on diabetes.** 2016.
2.   **National Diabetes Statistics Report.** 2017.
3.   Organization WH: **Classification of diabetes mellitus.** 2019.
4.   Kahn SE, Cooper ME, Del Prato S: **Pathophysiology and treatment of type 2 diabetes: perspectives on the past, present, and future.** *Lancet* 2014, **383:**1068-1083.
5.   Mooy JM, Grootenhuis PA, de Vries H, Valkenburg HA, Bouter LM, Kostense PJ, Heine RJ: **Prevalence and determinants of glucose intolerance in a Dutch caucasian population. The Hoorn Study.** *Diabetes Care* 1995, **18:**1270-1273.
6.   Stumvoll M, Goldstein BJ, van Haeften TW: **Type 2 diabetes: principles of pathogenesis and therapy.** *Lancet* 2005, **365:**1333-1346.
7.   Perl S, Kushner JA, Buchholz BA, Meeker AK, Stein GM, Hsieh M, Kirby M, Pechhold S, Liu EH, Harlan DM, Tisdale JF: **Significant human beta-cell turnover is limited to the first three decades of life as determined by in vivo thymidine analog incorporation and radiocarbon dating.** *J Clin Endocrinol Metab* 2010, **95:**E234-239.
8.   Brownlee M: **The pathobiology of diabetic complications: a unifying mechanism.** *Diabetes* 2005, **54:**1615-1625.
9.   Chung SS, Ho EC, Lam KS, Chung SK: **Contribution of polyol pathway to diabetes-induced oxidative stress.** *J Am Soc Nephrol* 2003, **14:**S233-236.
10.   Brownlee M: **Advanced protein glycosylation in diabetes and aging.** *Annu Rev Med* 1995, **46:**223-234.
11.   Kay AM, Simpson CL, Stewart JA, Jr.: **The Role of AGE/RAGE Signaling in Diabetes-Mediated Vascular Calcification.** *J Diabetes Res* 2016, **2016:**6809703.
12.   Kuboki K, Jiang ZY, Takahara N, Ha SW, Igarashi M, Yamauchi T, Feener EP, Herbert TP, Rhodes CJ, King GL: **Regulation of endothelial constitutive nitric oxide synthase gene expression in endothelial cells and in vivo : a specific vascular action of insulin.** *Circulation* 2000, **101:**676-681.
13.   Brownlee M: **Biochemistry and molecular cell biology of diabetic complications.** *Nature* 2001, **414:**813-820.
14.   Babik B, Petak F, Agocs S, Blaskovics I, Alacs E, Bodo K, Sudy R: **[Diabetes mellitus: endothelial dysfunction and changes in hemostasis].** *Orv Hetil* 2018, **159:**1335-1345.
15.   Williams B, Gallacher B, Patel H, Orme C: **Glucose-induced protein kinase C activation regulates vascular permeability factor mRNA expression and peptide production by human vascular smooth muscle cells in vitro.** *Diabetes* 1997, **46:**1497-1503.
16.   Shi Y, Vanhoutte PM: **Macro- and microvascular endothelial dysfunction in diabetes.** *J Diabetes* 2017, **9:**434-449.
17.   Fong DS, Aiello LP, Ferris FL, 3rd, Klein R: **Diabetic retinopathy.** *Diabetes Care* 2004, **27:**2540-2553.
18.   Fowler MJ: **Microvascular and Macrovascular Complications of Diabetes.** *Clinical Diabetes* 2011, **29:**116-122.
19.   Sandler M: **Is the lung a 'target organ' in diabetes mellitus?** *Arch Intern Med* 1990, **150:**1385-1388.
20.   Klein OL, Krishnan JA, Glick S, Smith LJ: **Systematic review of the association between lung function and Type 2 diabetes mellitus.** *Diabet Med* 2010, **27:**977-987.
21.   Lecube A, Simo R, Pallayova M, Punjabi NM, Lopez-Cano C, Turino C, Hernandez C, Barbe F: **Pulmonary Function and Sleep Breathing: Two New Targets for Type 2 Diabetes Care.** *Endocr Rev* 2017, **38:**550-573.

22. Barrett EJ, Liu Z, Khamaisi M, King GL, Klein R, Klein BEK, Hughes TM, Craft S, Freedman BI, Bowden DW, et al: **Diabetic Microvascular Disease: An Endocrine Society Scientific Statement.** *J Clin Endocrinol Metab* 2017, **102:**4343-4410.

23. Goldman MD: **Lung dysfunction in diabetes.** *Diabetes Care* 2003, **26:**1915-1918.

24. van den Borst B, Gosker HR, Zeegers MP, Schols AM: **Pulmonary function in diabetes: a metaanalysis.** *Chest* 2010, **138:**393-406.

25. Davis TM, Knuiman M, Kendall P, Vu H, Davis WA: **Reduced pulmonary function and its associations in type 2 diabetes: the Fremantle Diabetes Study.** *Diabetes Res Clin Pract* 2000, **50:**153-159.

26. McClean KM, Kee F, Young IS, Elborn JS: **Obesity and the lung: 1. Epidemiology.** *Thorax* 2008, **63:**649-654.

27. Cai D, Yuan M, Frantz DF, Melendez PA, Hansen L, Lee J, Shoelson SE: **Local and systemic insulin resistance resulting from hepatic activation of IKK-beta and NF-kappaB.** *Nat Med* 2005, **11:**183-190.

28. Arkan MC, Hevener AL, Greten FR, Maeda S, Li ZW, Long JM, Wynshaw-Boris A, Poli G, Olefsky J, Karin M: **IKK-beta links inflammation to obesity-induced insulin resistance.** *Nat Med* 2005, **11:**191-198.

29. Saidullah B, Muralidhar K, Fahim M: **Onset of diabetes modulates the airway smooth muscle reactivity of guinea pigs: role of epithelial mediators.** *J Smooth Muscle Res* 2014, **50:**29-38.

30. Martins JO, Wittlin BM, Anger DB, Martins DO, Sannomiya P, Jancar S: **Early phase of allergic airway inflammation in diabetic rats: role of insulin on the signaling pathways and mediators.** *Cell Physiol Biochem* 2010, **26:**739-748.

31. Cayir A, Ugan RA, Albayrak A, Kose D, Akpinar E, Cayir Y, Atmaca HT, Bayraktutan Z, Kara M: **The lung endothelin system: a potent therapeutic target with bosentan for the amelioration of lung alterations in a rat model of diabetes mellitus.** *J Endocrinol Invest* 2015, **38:**987-998.

32. Cazzola M, Calzetta L, Rogliani P, Lauro D, Novelli L, Page CP, Kanabar V, Matera MG: **High glucose enhances responsiveness of human airways smooth muscle via the Rho/ROCK pathway.** *Am J Respir Cell Mol Biol* 2012, **47:**509-516.

33. Gosens R, Nelemans SA, Hiemstra M, Grootte Bromhaar MM, Meurs H, Zaagsma J: **Insulin induces a hypercontractile airway smooth muscle phenotype.** *Eur J Pharmacol* 2003, **481:**125-131.

34. Ofulue AF, Thurlbeck WM: **Experimental diabetes and the lung. II. In vivo connective tissue metabolism.** *Am Rev Respir Dis* 1988, **138:**284-289.

35. Hollenbach J, Lopez-Rodriguez E, Muhlfeld C, Schipke J: **Voluntary Activity Modulates Sugar-Induced Elastic Fiber Remodeling in the Alveolar Region of the Mouse Lung.** *Int J Mol Sci* 2019, **20**.

36. Foster DJ, Ravikumar P, Bellotto DJ, Unger RH, Hsia CC: **Fatty diabetic lung: altered alveolar structure and surfactant protein expression.** *Am J Physiol Lung Cell Mol Physiol* 2010, **298:**L392-403.

37. Sugahara K, Ezaki K, Kaneko T, Morioka T, Maeda H: **Studies of the lungs in diabetes mellitus. II. Phospholipid analyses on the surfactant from broncho-alveolar lavage fluid of alloxan-induced diabetic rats.** *Biochem Biophys Res Commun* 1981, **98:**163-168.

38. Rehman Khan A, Awan FR: **Leptin Resistance: A Possible Interface Between Obesity and Pulmonary-Related Disorders.** *Int J Endocrinol Metab* 2016, **14:**e32586.

39. Zochodne DW: **Diabetes mellitus and the peripheral nervous system: manifestations and mechanisms.** *Muscle Nerve* 2007, **36:**144-166.

40. Bottini P, Scionti L, Santeusanio F, Casucci G, Tantucci C: **Impairment of the respiratory system in diabetic autonomic neuropathy.** *Diabetes Nutr Metab* 2000, **13:**165-172.

41. Martin-Frias M, Lamas A, Lara E, Alonso M, Ros P, Barrio R: **Pulmonary function in children with type 1 diabetes mellitus.** *J Pediatr Endocrinol Metab* 2015, **28:**163-169.

42. Schnapf BM, Banks RA, Silverstein JH, Rosenbloom AL, Chesrown SE, Loughlin GM: **Pulmonary function in insulin-dependent diabetes mellitus with limited joint mobility.** *Am Rev Respir Dis* 1984, **130:**930-932.

43. Wanke T, Formanek D, Auinger M, Popp W, Zwick H, Irsigler K: **Inspiratory muscle performance and pulmonary function changes in insulin-dependent diabetes mellitus.** *Am Rev Respir Dis* 1991, **143:**97-100.

44. Kuziemski K, Slominski W, Jassem E: **Impact of diabetes mellitus on functional exercise capacity and pulmonary functions in patients with diabetes and healthy persons.** *BMC Endocr Disord* 2019, **19:**2.

45. van Gent R, Brackel HJ, de Vroede M, van der Ent CK: **Lung function abnormalities in children with type I diabetes.** *Respir Med* 2002, **96:**976-978.

46. Antonelli Incalzi R, Fuso L, Giordano A, Pitocco D, Maiolo C, Calcagni ML, Ghirlanda G: **Neuroadrenergic denervation of the lung in type I diabetes mellitus complicated by autonomic neuropathy.** *Chest* 2002, **121:**443-451.

47. Bertherat J, Lubetzki J, Lockhart A, Regnard J: **Decreased bronchial response to methacholine in IDDM patients with autonomic neuropathy.** *Diabetes* 1991, **40:**1100-1106.

48. Mancini M, Filippelli M, Seghieri G, Iandelli I, Innocenti F, Duranti R, Scano G: **Respiratory muscle function and hypoxic ventilatory control in patients with type I diabetes.** *Chest* 1999, **115:**1553-1562.

49. Eaton T, Withy S, Garrett JE, Mercer J, Whitlock RM, Rea HH: **Spirometry in primary care practice: the importance of quality assurance and the impact of spirometry workshops.** *Chest* 1999, **116:**416-423.

50. Giner J, Plaza V, Rigau J, Sola J, Bolibar I, Sanchis J: **Spirometric standards and patient characteristics: an exploratory study of factors affecting fulfillment in routine clinical practice.** *Respir Care* 2014, **59:**1832-1837.

51. Scano G, Seghieri G, Mancini M, Filippelli M, Duranti R, Fabbri A, Innocenti F, Iandelli I, Misuri G: **Dyspnoea, peripheral airway involvement and respiratory muscle effort in patients with type I diabetes mellitus under good metabolic control.** *Clin Sci (Lond)* 1999, **96:**499-506.

52. Sahebjami H, Denholm D: **Effects of streptozotocin-induced diabetes on lung mechanics and biochemistry in rats.** *J Appl Physiol (1985)* 1988, **64:**147-153.

53. Beckman JA, Creager MA, Libby P: **Diabetes and atherosclerosis: epidemiology, pathophysiology, and management.** *JAMA* 2002, **287:**2570-2581.

54. Cheng G, Huang C, Deng H, Wang H: **Diabetes as a risk factor for dementia and mild cognitive impairment: a meta-analysis of longitudinal studies.** *Intern Med J* 2012, **42:**484-491.

55. Cipolla MJ: In *The Cerebral Circulation.* San Rafael (CA); 2009: *Integrated Systems Physiology: From Molecule to Function*].

56. Paulson OB, Strandgaard S, Edvinsson L: **Cerebral autoregulation.** *Cerebrovasc Brain Metab Rev* 1990, **2:**161-192.

57. Phillips SJ, Whisnant JP: **Hypertension and the brain. The National High Blood Pressure Education Program.** *Arch Intern Med* 1992, **152:**938-945.

58. Faraci FM, Heistad DD: **Regulation of large cerebral arteries and cerebral microvascular pressure.** *Circ Res* 1990, **66:**8-17.

59. Miller FJ, Jr., Dellsperger KC, Gutterman DD: **Myogenic constriction of human coronary arterioles.** *Am J Physiol* 1997, **273:**H257-264.

60. Davis MJ: **Myogenic response gradient in an arteriolar network.** *Am J Physiol* 1993, **264:**H2168-2179.

61. Cipolla MJ, Curry AB: **Middle cerebral artery function after stroke: the threshold duration of reperfusion for myogenic activity.** *Stroke* 2002, **33:**2094-2099.

62. Aukes AM, Bishop N, Godfrey J, Cipolla MJ: **The influence of pregnancy and gender on perivascular innervation of rat posterior cerebral arteries.** *Reprod Sci* 2008, **15:**411-419.

63. Girouard H, Iadecola C: **Neurovascular coupling in the normal brain and in hypertension, stroke, and Alzheimer disease.** *J Appl Physiol (1985)* 2006, **100:**328-335.

64. Iadecola C, Nedergaard M: **Glial regulation of the cerebral microvasculature.** *Nat Neurosci* 2007, **10:**1369-1376.

65. Phillips AA, Chan FH, Zheng MM, Krassioukov AV, Ainslie PN: **Neurovascular coupling in humans: Physiology, methodological advances and clinical implications.** *J Cereb Blood Flow Metab* 2016, **36:**647-664.

66. Coucha M, Abdelsaid M, Ward R, Abdul Y, Ergul A: **Impact of Metabolic Diseases on Cerebral Circulation: Structural and Functional Consequences.** *Compr Physiol* 2018, **8:**773-799.

67. Bentsen N, Larsen B, Lassen NA: **Chronically impaired autoregulation of cerebral blood flow in long-term diabetics.** *Stroke* 1975, **6:**497-502.

68. Xu RS: **Pathogenesis of diabetic cerebral vascular disease complication.** *World J Diabetes* 2015, **6:**54-66.

69. Shirahase H, Usui H, Kurahashi K, Fujiwara M, Fukui K: **Possible role of endothelial thromboxane A2 in the resting tone and contractile responses to acetylcholine and arachidonic acid in canine cerebral arteries.** *J Cardiovasc Pharmacol* 1987, **10:**517-522.

70. Poston L, Taylor PD: **Glaxo/MRS Young Investigator Prize. Endothelium-mediated vascular function in insulin-dependent diabetes mellitus.** *Clin Sci (Lond)* 1995, **88:**245-255.

71. Sauve M, Hui SK, Dinh DD, Foltz WD, Momen A, Nedospasov SA, Offermanns S, Husain M, Kroetsch JT, Lidington D, Bolz SS: **Tumor Necrosis Factor/Sphingosine-1-Phosphate Signaling Augments Resistance Artery Myogenic Tone in Diabetes.** *Diabetes* 2016, **65:**1916-1928.

72. Casella S, Bielli A, Mauriello A, Orlandi A: **Molecular Pathways Regulating Macrovascular Pathology and Vascular Smooth Muscle Cells Phenotype in Type 2 Diabetes.** *Int J Mol Sci* 2015, **16:**24353-24368.

73. Zimmermann PA, Knot HJ, Stevenson AS, Nelson MT: **Increased myogenic tone and diminished responsiveness to ATP-sensitive K+ channel openers in cerebral arteries from diabetic rats.** *Circ Res* 1997, **81:**996-1004.

74. Abd-Elrahman KS, Walsh MP, Cole WC: **Abnormal Rho-associated kinase activity contributes to the dysfunctional myogenic response of cerebral arteries in type 2 diabetes.** *Can J Physiol Pharmacol* 2015, **93:**177-184.

75. Cole WC, Welsh DG: **Role of myosin light chain kinase and myosin light chain phosphatase in the resistance arterial myogenic response to intravascular pressure.** *Arch Biochem Biophys* 2011, **510:**160-173.

76. Erdos B, Snipes JA, Miller AW, Busija DW: **Cerebrovascular dysfunction in Zucker obese rats is mediated by oxidative stress and protein kinase C.** *Diabetes* 2004, **53:**1352-1359.

77. Elgebaly MM, Prakash R, Li W, Ogbi S, Johnson MH, Mezzetti EM, Fagan SC, Ergul A: **Vascular protection in diabetic stroke: role of matrix metalloprotease-dependent vascular remodeling.** *J Cereb Blood Flow Metab* 2010, **30:**1928-1938.

78. Endemann DH, Pu Q, De Ciuceis C, Savoia C, Virdis A, Neves MF, Touyz RM, Schiffrin EL: **Persistent remodeling of resistance arteries in type 2 diabetic patients on antihypertensive treatment.** *Hypertension* 2004, **43:**399-404.

79. Ergul A, Valenzuela JP, Fouda AY, Fagan SC: **Cellular connections, microenvironment and brain angiogenesis in diabetes: Lost communication signals in the post-stroke period.** *Brain Res* 2015, **1623:**81-96.

80. Sweeney MD, Ayyadurai S, Zlokovic BV: **Pericytes of the neurovascular unit: key functions and signaling pathways.** *Nat Neurosci* 2016, **19:**771-783.

81. Fulesdi B, Limburg M, Bereczki D, Michels RP, Neuwirth G, Legemate D, Valikovics A, Csiba L: **Impairment of cerebrovascular reactivity in long-term type 1 diabetes.** *Diabetes* 1997, **46:**1840-1845.

82. Fulesdi B, Limburg M, Bereczki D, Molnar C, Michels RP, Leanyvari Z, Csiba L: **No relationship between cerebral blood flow velocity and cerebrovascular reserve capacity and contemporaneously measured glucose and insulin concentrations in diabetes mellitus.** *Acta Diabetol* 1999, **36:**191-195.

83. Hidasi E, Kaplar M, Dioszeghy P, Bereczki D, Csiba L, Limburg M, Fulesdi B: **No correlation between impairment of cerebrovascular reserve capacity and electrophysiologically assessed severity of neuropathy in noninsulin-dependent diabetes mellitus.** *J Diabetes Complications* 2002, **16:**228-234.

84. Siro P, Molnar C, Katona E, Antek C, Kollar J, Settakis G, Fulesdi B: **Carotid intima-media thickness and cerebrovascular reactivity in long-term type 1 diabetes mellitus.** *J Clin Ultrasound* 2009, **37:**451-456.

85. Starr JM, Wardlaw J, Ferguson K, MacLullich A, Deary IJ, Marshall I: **Increased blood-brain barrier permeability in type II diabetes demonstrated by gadolinium magnetic resonance imaging.** *J Neurol Neurosurg Psychiatry* 2003, **74:**70-76.

86. Armulik A, Abramsson A, Betsholtz C: **Endothelial/pericyte interactions.** *Circ Res* 2005, **97:**512-523.

87. Raza S, Blackstone EH, Sabik JF, 3rd: **The diabetes epidemic and its effect on cardiac surgery practice.** *J Thorac Cardiovasc Surg* 2015, **150:**783-784.

88. Khunti K, Wolden ML, Thorsted BL, Andersen M, Davies MJ: **Clinical inertia in people with type 2 diabetes: a retrospective cohort study of more than 80,000 people.** *Diabetes Care* 2013, **36:**3411-3417.

89. Feener EP, King GL: **Vascular dysfunction in diabetes mellitus.** *Lancet* 1997, **350 Suppl 1:**SI9-13.

90. Morricone L, Ranucci M, Denti S, Cazzaniga A, Isgro G, Enrini R, Caviezel F: **Diabetes and complications after cardiac surgery: comparison with a non-diabetic population.** *Acta Diabetol* 1999, **36:**77-84.

91. Fulesdi B, Limburg M, Bereczki D, Kaplar M, Molnar C, Kappelmayer J, Neuwirth G, Csiba L: **Cerebrovascular reactivity and reserve capacity in type II diabetes mellitus.** *J Diabetes Complications* 1999, **13:**191-199.

92. Perez-Belmonte LM, San Roman-Teran CM, Jimenez-Navarro M, Barbancho MA, Garcia-Alberca JM, Lara JP: **Assessment of long-term cognitive impairment after off-pump coronary-artery bypass grafting and related risk factors.** *J Am Med Dir Assoc* 2015, **16:**263 e269-211.

93. Notzold A, Michel K, Khattab AA, Sievers HH, Huppe M: **Diabetes mellitus increases adverse neurocognitive outcome after coronary artery bypass grafting surgery.** *Thorac Cardiovasc Surg* 2006, **54:**307-312.

94. Bucerius J, Gummert JF, Borger MA, Walther T, Doll N, Onnasch JF, Metz S, Falk V, Mohr FW: **Stroke after cardiac surgery: a risk factor analysis of 16,184 consecutive adult patients.** *Ann Thorac Surg* 2003, **75:**472-478.

95. Kadoi Y, Goto F: **Factors associated with postoperative cognitive dysfunction in patients undergoing cardiac surgery.** *Surg Today* 2006, **36:**1053-1057.

96. Walley KR: **Use of central venous oxygen saturation to guide therapy.** *Am J Respir Crit Care Med* 2011, **184:**514-520.

97. Dueck MH, Klimek M, Appenrodt S, Weigand C, Boerner U: **Trends but not individual values of central venous oxygen saturation agree with mixed venous oxygen saturation during varying hemodynamic conditions.** *Anesthesiology* 2005, **103:**249-257.

98. Barret K, Barman S, Boitano S, Brooks H: **Circulation Through Special Regions.** In *Ganong's Review of Medical Physiology.* New York: McGraw-Hill Companies, Inc; 2010: 569-585

99. Kadoi Y, Saito S, Kawahara F, Goto F, Owada R, Fujita N: **Jugular venous bulb oxygen saturation in patients with preexisting diabetes mellitus or stroke during normothermic cardiopulmonary bypass.** *Anesthesiology* 2000, **92:**1324-1329.

100. Hill MD: **Stroke and diabetes mellitus.** *Handb Clin Neurol* 2014, **126:**167-174.

101. Molehin OR, Oloyede OI, Adefegha SA: **Streptozotocin-induced diabetes in rats: effects of White Butterfly (Clerodendrum volubile) leaves on blood glucose levels, lipid profile and antioxidant status.** *Toxicol Mech Methods* 2018, **28:**573-586.

102. Reed MJ, Meszaros K, Entes LJ, Claypool MD, Pinkett JG, Gadbois TM, Reaven GM: **A new rat model of type 2 diabetes: the fat-fed, streptozotocin-treated rat.** *Metabolism* 2000, **49:**1390-1394.

103. Skovso S: **Modeling type 2 diabetes in rats using high fat diet and streptozotocin.** *J Diabetes Investig* 2014, **5:**349-358.

104. Srinivasan K, Viswanad B, Asrat L, Kaul CL, Ramarao P: **Combination of high-fat diet-fed and low-dose streptozotocin-treated rat: a model for type 2 diabetes and pharmacological screening.** *Pharmacol Res* 2005, **52:**313-320.

105. Tancrede G, Rousseau-Migneron S, Nadeau A: **Long-term changes in the diabetic state induced by different doses of streptozotocin in rats.** *Br J Exp Pathol* 1983, **64:**117-123.

106. Zhang M, Lv XY, Li J, Xu ZG, Chen L: **The characterization of high-fat diet and multiple low-dose streptozotocin induced type 2 diabetes rat model.** *Exp Diabetes Res* 2008, **2008:**704045.

107. Janosi TZ, Adamicza A, Zosky GR, Asztalos T, Sly PD, Hantos Z: **Plethysmographic estimation of thoracic gas volume in apneic mice.** *J Appl Physiol (1985)* 2006, **101:**454-459.

108. Petak F, Hantos Z, Adamicza A, Asztalos T, Sly PD: **Methacholine-induced bronchoconstriction in rats: effects of intravenous vs. aerosol delivery.** *J Appl Physiol (1985)* 1997, **82:**1479-1487.

109. Hantos Z, Daroczy B, Suki B, Nagy S, Fredberg JJ: **Input impedance and peripheral inhomogeneity of dog lungs.** *J Appl Physiol (1985)* 1992, **72:**168-178.

110. Fredberg JJ, Stamenovic D: **On the imperfect elasticity of lung tissue.** *J Appl Physiol (1985)* 1989, **67:**2408-2419.

111. Berggren S: **The oxygen deficit of arterial blood caused by non-ventilating parts of the lung.** *Acta Physiol Scand* 1942, **4**.

112. Schindelin J, Arganda-Carreras I, Frise E, Kaynig V, Longair M, Pietzsch T, Preibisch S, Rueden C, Saalfeld S, Schmid B, et al: **Fiji: an open-source platform for biological-image analysis.** *Nat Methods* 2012, **9:**676-682.

113. Scholkmann F, Kleiser S, Metz AJ, Zimmermann R, Mata Pavia J, Wolf U, Wolf M: **A review on continuous wave functional near-infrared spectroscopy and imaging instrumentation and methodology.** *Neuroimage* 2014, **85 Pt 1:**6-27.

114. Owen-Reece H, Smith M, Elwell CE, Goldstone JC: **Near infrared spectroscopy.** *Br J Anaesth* 1999, **82:**418-426.

115. Gregory AJ, Hatem MA, Yee K, Grocott HP: **Optimal Placement of Cerebral Oximeter Monitors to Avoid the Frontal Sinus as Determined by Computed Tomography.** *J Cardiothorac Vasc Anesth* 2016, **30:**127-133.

116. R. Barker Bausell Y-FL: *Power Analysis for Experimental Research: A Practical Guide for the Biological, Medical and Social Sciences.* Cambridge: Cambridge University Press; 2002.

117. Jargen P, Dietrich A, Herling AW, Hammes HP, Wohlfart P: **The role of insulin resistance in experimental diabetic retinopathy-Genetic and molecular aspects.** *PLoS One* 2017, **12:**e0178658.

118. Chao PC, Li Y, Chang CH, Shieh JP, Cheng JT, Cheng KC: **Investigation of insulin resistance in the popularly used four rat models of type-2 diabetes.** *Biomed Pharmacother* 2018, **101:**155-161.

119. Douglas NJ, Campbell IW, Ewing DJ, Clarke BF, Flenley DC: **Reduced airway vagal tone in diabetic patients with autonomic neuropathy.** *Clin Sci (Lond)* 1981, **61:**581-584.

120. Oliveira TL, Candeia-Medeiros N, Cavalcante-Araujo PM, Melo IS, Favaro-Pipi E, Fatima LA, Rocha AA, Goulart LR, Machado UF, Campos RR, Sabino-Silva R: **SGLT1 activity in lung alveolar cells of diabetic rats modulates airway surface liquid glucose concentration and bacterial proliferation.** *Sci Rep* 2016, **6:**21752.

121. Duncan BB, Schmidt MI, Pankow JS, Ballantyne CM, Couper D, Vigo A, Hoogeveen R, Folsom AR, Heiss G, Atherosclerosis Risk in Communities S: **Low-grade systemic inflammation and the development of type 2 diabetes: the atherosclerosis risk in communities study.** *Diabetes* 2003, **52:**1799-1805.

122. Schmidt MI, Duncan BB, Sharrett AR, Lindberg G, Savage PJ, Offenbacher S, Azambuja MI, Tracy RP, Heiss G: **Markers of inflammation and prediction of diabetes mellitus in adults (Atherosclerosis Risk in Communities study): a cohort study.** *Lancet* 1999, **353:**1649-1652.

123. Singh S, Bodas M, Bhatraju NK, Pattnaik B, Gheware A, Parameswaran PK, Thompson M, Freeman M, Mabalirajan U, Gosens R, et al: **Hyperinsulinemia adversely affects lung structure and function.** *Am J Physiol Lung Cell Mol Physiol* 2016, **310:**L837-845.

124. Wang CC, Gurevich I, Draznin B: **Insulin affects vascular smooth muscle cell phenotype and migration via distinct signaling pathways.** *Diabetes* 2003, **52:**2562-2569.

125. Verrotti A, Verini M, Chiarelli F, Verdesca V, Misticoni G, Morgese G: **Pulmonary function in diabetic children with and without persistent microalbuminuria.** *Diabetes Res Clin Pract* 1993, **21:**171-176.

126. Faffe DS, Zin WA: **Lung parenchymal mechanics in health and disease.** *Physiol Rev* 2009, **89:**759-775.

127. Suki B, Ito S, Stamenovic D, Lutchen KR, Ingenito EP: **Biomechanics of the lung parenchyma: critical roles of collagen and mechanical forces.** *J Appl Physiol (1985)* 2005, **98:**1892-1899.

128. Suki B, Bates JH: **Lung tissue mechanics as an emergent phenomenon.** *J Appl Physiol (1985)* 2011, **110:**1111-1118.

129. Hu Y, Ma Z, Guo Z, Zhao F, Wang Y, Cai L, Yang J: **Type 1 diabetes mellitus is an independent risk factor for pulmonary fibrosis.** *Cell Biochem Biophys* 2014, **70:**1385-1391.

130. Ogurtsova K, da Rocha Fernandes JD, Huang Y, Linnenkamp U, Guariguata L, Cho NH, Cavan D, Shaw JE, Makaroff LE: **IDF Diabetes Atlas: Global estimates for the prevalence of diabetes for 2015 and 2040.** *Diabetes Res Clin Pract* 2017, **128:**40-50.

131. Collaboration NCDRF: **Worldwide trends in diabetes since 1980: a pooled analysis of 751 population-based studies with 4.4 million participants.** *Lancet* 2016, **387:**1513-1530.

132. Lee MJ, Coast JR, Hempleman SC, Baldi JC: **Type 1 Diabetes Duration Decreases Pulmonary Diffusing Capacity during Exercise.** *Respiration* 2016, **91:**164-170.

133. Grinnan D, Farr G, Fox A, Sweeney L: **The Role of Hyperglycemia and Insulin Resistance in the Development and Progression of Pulmonary Arterial Hypertension.** *J Diabetes Res* 2016, **2016:**2481659.

134. Vracko R, Thorning D, Huang TW: **Basal lamina of alveolar epithelium and capillaries: quantitative changes with aging and in diabetes mellitus.** *Am Rev Respir Dis* 1979, **120:**973-983.

135. Vinik AI, Maser RE, Mitchell BD, Freeman R: **Diabetic autonomic neuropathy.** *Diabetes Care* 2003, **26:**1553-1579.

136. Belmonte KE, Fryer AD, Costello RW: **Role of insulin in antigen-induced airway eosinophilia and neuronal M2 muscarinic receptor dysfunction.** *J Appl Physiol (1985)* 1998, **85:**1708-1718.

137. Talakatta G, Sarikhani M, Muhamed J, Dhanya K, Somashekar BS, Mahesh PA, Sundaresan N, Ravindra PV: **Diabetes induces fibrotic changes in the lung through the activation of TGF-beta signaling pathways.** *Sci Rep* 2018, **8:**11920.

138. Halayko AJ, Tran T, Gosens R: **Phenotype and functional plasticity of airway smooth muscle: role of caveolae and caveolins.** *Proc Am Thorac Soc* 2008, **5:**80-88.

139. Carvalho VF, Barreto EO, Arantes ACS, Serra MF, Ferreira TPT, Jannini-Sa YAP, Hogaboam CM, Martins MA, Silva PMR: **Diabetes Downregulates Allergen-Induced Airway Inflammation in Mice.** *Mediators Inflamm* 2018, **2018:**6150843.

140. Kolahian S, Asadi F, Nassiri SM: **Airway inflammatory events in diabetic-antigen sensitized guinea pigs.** *Eur J Pharmacol* 2011, **659:**252-258.

141. Rhind GB, Gould GA, Ewing DJ, Clarke BF, Douglas NJ: **Increased bronchial reactivity to histamine in diabetic autonomic neuropathy.** *Clin Sci (Lond)* 1987, **73:**401-405.

142. Golic M, Walsh K, Lawson P: **Short-wavelength near-infrared spectra of sucrose, glucose, and fructose with respect to sugar concentration and temperature.** *Appl Spectrosc* 2003, **57:**139-145.

143. Maier JS, Walker SA, Fantini S, Franceschini MA, Gratton E: **Possible correlation between blood glucose concentration and the reduced scattering coefficient of tissues in the near infrared.** *Opt Lett* 1994, **19:**2062-2064.

144. Rask-Madsen C, King GL: **Vascular complications of diabetes: mechanisms of injury and protective factors.** *Cell Metab* 2013, **17:**20-33.

145. Sena CM, Pereira AM, Seica R: **Endothelial dysfunction - a major mediator of diabetic vascular disease.** *Biochim Biophys Acta* 2013, **1832:**2216-2231.

146. Westein E, Hoefer T, Calkin AC: **Thrombosis in diabetes: a shear flow effect?** *Clin Sci (Lond)* 2017, **131:**1245-1260.

147. Miyoshi S, Morita T, Kadoi Y, Goto F: **Analysis of the factors related to a decrease in jugular venous oxygen saturation in patients with diabetes mellitus during normothermic cardiopulmonary bypass.** *Surg Today* 2005, **35:**530-534.

148. Kadoi Y, Saito S, Goto F, Someya T, Kamiyashiki S, Fujita N: **Time course of changes in jugular venous oxygen saturation during hypothermic or normothermic cardiopulmonary bypass in patients with diabetes mellitus.** *Acta Anaesthesiol Scand* 2001, **45:**858-862.

149. Oh YJ, Kim JY, Shim JK, Yoo KJ, Lee JW, Kwak YL: **Diabetes mellitus does not affect jugular bulb oxygen saturation in patients undergoing off-pump coronary artery bypass graft surgery.** *Circ J* 2008, **72:**1259-1264.

150. Baikoussis NG, Karanikolas M, Siminelakis S, Matsagas M, Papadopoulos G: **Baseline cerebral oximetry values in cardiac and vascular surgery patients: a prospective observational study.** *J Cardiothorac Surg* 2010, **5:**41.

151. Drury PP, Gunn AJ, Bennet L, Ganeshalingham A, Finucane K, Buckley D, Beca J: **Deep hypothermic circulatory arrest during the arterial switch operation is associated with reduction in cerebral oxygen extraction but no increase in white matter injury.** *J Thorac Cardiovasc Surg* 2013, **146:**1327-1333.

152. Ono M, Brady K, Easley RB, Brown C, Kraut M, Gottesman RF, Hogue CW, Jr.: **Duration and magnitude of blood pressure below cerebral autoregulation threshold during cardiopulmonary bypass is associated with major morbidity and operative mortality.** *J Thorac Cardiovasc Surg* 2014, **147:**483-489.

153. Kowalewski M, Pawliszak W, Malvindi PG, Bokszanski MP, Perlinski D, Raffa GM, Kowalkowska ME, Zaborowska K, Navarese EP, Kolodziejczak M, et al: **Off-pump coronary artery bypass grafting improves short-term outcomes in high-risk patients compared with on-pump coronary artery bypass grafting: Meta-analysis.** *J Thorac Cardiovasc Surg* 2016, **151:**60-77 e61-58.

154. Sun JH, Wu XY, Wang WJ, Jin LL: **Cognitive dysfunction after off-pump versus on-pump coronary artery bypass surgery: a meta-analysis.** *J Int Med Res* 2012, **40:**852-858.

155. Willie CK, Tzeng YC, Fisher JA, Ainslie PN: **Integrative regulation of human brain blood flow.** *J Physiol* 2014, **592:**841-859.

156. Bickler PE, Feiner JR, Rollins MD: **Factors affecting the performance of 5 cerebral oximeters during hypoxia in healthy volunteers.** *Anesth Analg* 2013, **117:**813-823.

157. Moerman A, Wouters P: **Near-infrared spectroscopy (NIRS) monitoring in contemporary anesthesia and critical care.** *Acta Anaesthesiol Belg* 2010, **61:**185-194.

158. Bevan PJ: **Should Cerebral Near-infrared Spectroscopy be Standard of Care in Adult Cardiac Surgery?** *Heart Lung Circ* 2015, **24:**544-550.

159. Green MS, Sehgal S, Tariq R: **Near-Infrared Spectroscopy: The New Must Have Tool in the Intensive Care Unit?** *Semin Cardiothorac Vasc Anesth* 2016, **20:**213-224.

160. Rescoe E, Tang X, Perry DA, Sleeper LA, DiNardo JA, Kussman BD, Kheir JN: **Cerebral near-infrared spectroscopy insensitively detects low cerebral venous oxygen saturations after stage 1 palliation.** *J Thorac Cardiovasc Surg* 2017, **154:**1056-1062.

161. Simons J, Sood ED, Derby CD, Pizarro C: **Predictive value of near-infrared spectroscopy on neurodevelopmental outcome after surgery for congenital heart disease in infancy.** *J Thorac Cardiovasc Surg* 2012, **143:**118-125.

162. Chan MJ, Chung T, Glassford NJ, Bellomo R: **Near-Infrared Spectroscopy in Adult Cardiac Surgery Patients: A Systematic Review and Meta-Analysis.** *J Cardiothorac Vasc Anesth* 2017, **31:**1155-1165.

163. Rogers CA, Stoica S, Ellis L, Stokes EA, Wordsworth S, Dabner L, Clayton G, Downes R, Nicholson E, Bennett S, et al: **Randomized trial of near-infrared spectroscopy for personalized optimization of cerebral tissue oxygenation during cardiac surgery.** *Br J Anaesth* 2017, **119:**384-393.

164.   Conway BA, Hultborn H, Kiehn O: **Proprioceptive input resets central locomotor rhythm in the spinal cat.** *Exp Brain Res* 1987, **68:**643-656.